Article

New Base Pairing Motifs. The Synthesis and Thermal Stability of Oligodeoxynucleotides Containing Imidazopyridopyrimidine Nucleosides with the Ability to Form Four Hydrogen Bonds

Noriaki Minakawa, Naoshi Kojima, Sadao Hikishima, Takashi Sasaki, Arihiro Kiyosue, Naoko Atsumi, Yoshihito Ueno, and Akira Matsuda

J. Am. Chem. Soc., **2003**, 125 (33), 9970-9982• DOI: 10.1021/ja0347686 • Publication Date (Web): 24 July 2003

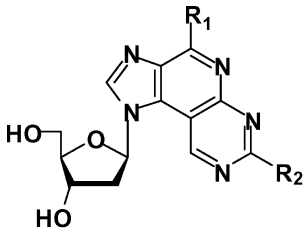

1: $R_1 = NH_2$, $R_2 = NH_2$
2: $R_1 = OH$, $R_2 = OH$
3: $R_1 = NH_2$, $R_2 = OH$
4: $R_1 = OH$, $R_2 = NH_2$

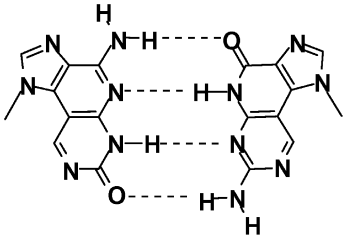

$N^O : O^N$ (+6 °C per modification)

More About This Article

Additional resources and features associated with this article are available within the HTML version:

- Supporting Information
- Links to the 4 articles that cite this article, as of the time of this article download
- Access to high resolution figures
- Links to articles and content related to this article
- Copyright permission to reproduce figures and/or text from this article

View the Full Text HTML

J|A|C|S
ARTICLES
Published on Web 07/24/2003

New Base Pairing Motifs. The Synthesis and Thermal Stability of Oligodeoxynucleotides Containing Imidazopyridopyrimidine Nucleosides with the Ability to Form Four Hydrogen Bonds

Noriaki Minakawa,* Naoshi Kojima, Sadao Hikishima, Takashi Sasaki, Arihiro Kiyosue, Naoko Atsumi, Yoshihito Ueno, and Akira Matsuda*

Contribution from the Graduate School of Pharmaceutical Sciences, Hokkaido University, Kita-12, Nishi-6, Kita-ku, Sapporo 060-0812, Japan

Received February 20, 2003; E-mail: noriaki@pharm.hokudai.ac.jp; matuda@pharm.hokudai.ac.jp

Abstract: The synthesis and thermal stability of oligodeoxynucleotides (ODNs) containing imidazo[5′,4′:4,5]pyrido[2,3-*d*]pyrimidine nucleosides **1**−**4** (**N^N**, **O^O**, **N^O**, and **O^N**, respectively) with the aim of developing two sets of new base pairing motifs consisting of four hydrogen bonds (H-bonds) is described. The proposed four tricyclic nucleosides **1**−**4** were synthesized through the Stille coupling reaction of a 5-iodoimidazole nucleoside with an appropriate 5-stannylpyrimidine derivative, followed by an intramolecular cyclization. These nucleosides were incorporated into ODNs to investigate the H-bonding ability. When one molecule of the tricyclic nucleosides was incorporated into the center of each ODN (ODN I and II, each 17mer), no apparent specificity of base pairing was observed, and all duplexes were less stable than the duplexes containing natural G:C and A:T pairs. On the other hand, when three molecules of the tricyclic nucleosides were consecutively incorporated into the center of each ODN (ODN III and IV, each 17mer), thermal and thermodynamic stabilization of the duplexes due to the specific base pairings was observed. The melting temperature (T_m) of the duplex containing the **N^O**:**O^N** pairs showed the highest T_m of 84.0 °C, which was 18.2 and 23.5 °C higher than that of the duplexes containing G:C and A:T pairs, respectively. This result implies that **N^O** and **O^N** form base pairs with four H-bonds when they are incorporated into ODNs. The duplex containing **N^O**:**O^N** pairs was markedly stabilized by the assistance of the stacking ability of the imidazopyridopyrimidine bases. Thus, we developed a thermally stable new base pairing motif, which should be useful for the stabilization and regulation of a variety of DNA structures.

Introduction

DNA, as is well-known, is the storage and carrier of genetic information in all living organisms and generally forms a right-handed double helix with a complementary DNA molecule. The structure of the DNA double helix is based on the Watson−Crick hydrogen bonding (H-bonding) of adenine:thymine (two H-bonds) and guanine:cytosine (three H-bonds) base pairings. H-bonding interaction plays a critical role in not only conserving and transmitting genetic information but also in double helix stability. In addition to the general right-handed double helix with a straight axis, DNA is also known to adopt a variety of structures including left-handed Z conformations, hairpins, cruciforms, branched junctions, and quadruplexes depending on their sequences and environmental conditions.[1] The foundation of the structures in these intra- and intermolecular interactions is not only Watson−Crick base pairing but also Hoogsteen type interactions.[2] Thus, H-bonding between nucleobases, as well as sequences, is thought to play a critical role in the conformational diversity of DNA, each of which would be essential for biological processes in cells. Consequently, much attention has been devoted to the synthesis of artificial oligodeoxynucleotides (ODNs) including unnatural nucleobases, which could form a more stable, higher-ordered structure with DNA, RNA and protein, or DNA itself, with application to biochemistry, biotechnology, and medicinal chemistry.[3] Their therapeutic application, for example, in antisense and antigene methodologies is an area of intense study, and a large number of ODNs have been synthesized and evaluated for the thermal stability of their duplex and triplex structures.[4] In contrast to the research directed toward thermally stable base pairing between natural and unnatural nucleobases, few studies have been reported on the possibility of alternative base pairing consisting of new H-bonding motifs.[3d,3f,5] For example, Benner et al. proposed new base pairing, that is, isoguanine:isocytosine (isoG:isoC) and 2,6-diaminopyrimidine:1-methyl-pyrazolo[4,3-*d*]pyrimidine-5,7(4*H*,6*H*)-dione base pairs, and investigated their enzymatic incorporation into DNA and RNA with the aim of "extending the genetic alphabet".[6] Although such effort has now been replaced by the development of a new base pairing motif through

(1) Recent reviews of conformation diversity, see (a) Lilley, D. M. J. In *Bioorganic Chemistry: Nucleic Acids*; Hecht, S. M., Ed.; Oxford University Press: Oxford, 1996; Ch. 7, pp 186−215. (b) Belmont, P.; Constant, J.-F.; Demeunynck, M. *Chem. Soc. Rev.* **2001**, *30*, 70−81.

(2) (a) Hoogsteen, K. *Acta Crystallogr.* **1963**, *16*, 907−916. (b) Quigley, G. J.; Ughetto, G.; van der Marel, G.; van Boom, J. H.; Wang, A. H.-J.; Rich, A. *Science* **1986**, *232*, 1255−1258.

10.1021/ja0347686 CCC: $25.00

hydrophobic interactions,[7] rather than H-bonding interactions, the results showing that the isoG:isoC bearing duplex has a thermal stability comparable to that of the corresponding guanine:cytosine base pair and is considerably greater than that of the adenine:uracil base pair[8] warrant consideration. Prompted by these results, we envisioned a new base pairing motif, which would be more thermally stable than the Watson−Crick H-bonding. To this end, we propose two sets of new base pair combinations consisting of four H-bonds, as shown in Figure 1.[9] Thus far, several investigations of ODNs, including the extended nucleobases, have been reported.[3e,j,n,4g,10] However, to our knowledge, there have been no reports with the goal of stabilizing and controlling not only helical structures but also other possible structures. Therefore, it seems worthwhile to examine the proposed new base pairing motif when these nucleobases are incorporated into complementary positions of ODNs. Since the tricyclic nucleobases have extended flat aromatic surfaces, enhancement of the stacking interaction is also expected.[11] In addition, the tricyclic skeletons also have a Hoogsteen type interaction ability as do natural purine bases,

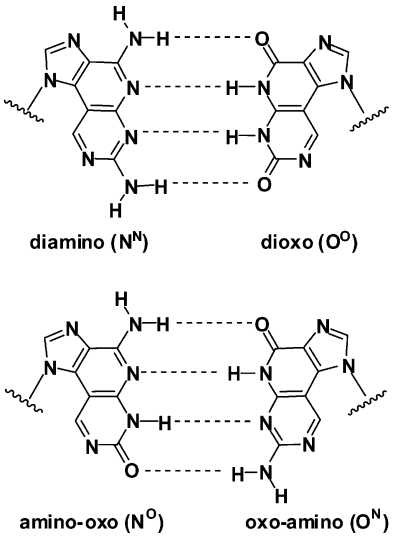

Figure 1. Proposed new base pairs consisting of four H-bonds.

Scheme 1 [a]

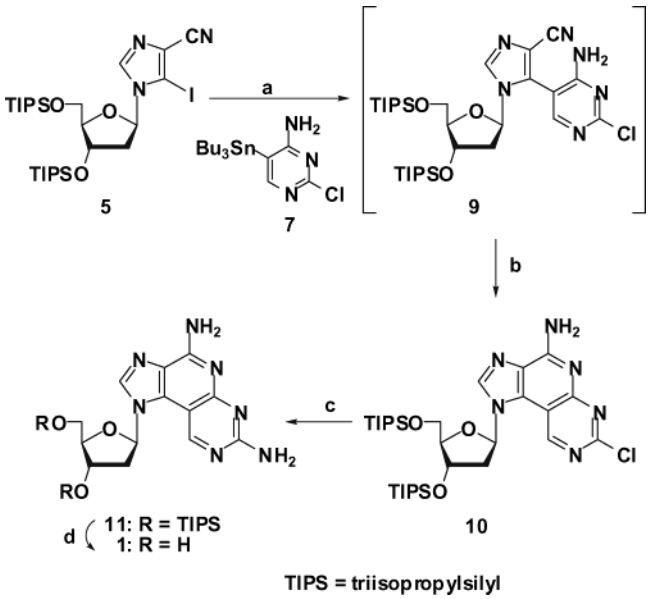

[a] Reagents: (a) $dba_3Pd_2{\cdot}CHCl_3$, DMF, 100 °C; (b) EtOH(aq) Na_2CO_3, 80 °C; (c) 1,4-dioxane-NH_4OH, 100 °C; and (d) TBAF, THF.

which may contribute to adopting the three-dimensional structures of ODNs.

In this paper, we describe the synthesis and incorporation of these tricyclic imidazopyridopyrimidine nucleosides into ODNs and their effects on thermal stabilities of the ODNs, including the newly designed base paring motifs.

Results and Discussion

1. Chemistry. The most straightforward synthesis of the desired nucleosides was thought to be through intramolecular cyclization of the 5-pyrimidinylimidazole nucleosides, which would be prepared from the Stille coupling reaction of a 5-iodoimidazole nucleoside with an appropriate tributylstannylpyrimidine. The 5-iodoimidazole nucleosides **5** (Scheme 1) and **6** (Scheme 3) can be synthesized from 2′-deoxyinosine.[12] On the other hand, the tributylstannylpyrimidine derivatives **7** and **8** can be synthesized from 2,4-dichloropyrimidine.[13] These chemical conversions are presented in the Supporting Information.[14]

(3) For examples except for antisense and antigene methodologies: (a) Goeddel, D. V.; Yansura, D. G.; Caruthers, M. H. *Proc. Natl. Acad. Sci. U.S.A.* **1978**, *75*, 3578−3582. (b) Taboury, J. A.; Adam, S.; Taillandier, E.; Neumann, J.-M.; Tran-Dinh, S.; Huynh-Dinh, T.; Langlois d'Estaintot, B.; Conti, M.; Igolen, J. *Nucleic Acids Res.* **1984**, *12*, 6291−6305. (c) Chollet, A.; Kawashima, E. *Nucleic Acids Res.* **1988**, *16*, 305−317. (d) Solomon, M. S.; Hopkins, P. B. *J. Org. Chem.* **1993**, *58*, 2232−2243. (e) Langouet, S.; Muller, M.; Guengerich, F. P. *Biochemistry* **1997**, *36*, 6069−6079. (f) Beaussire, J.-J.; Pochet, S. *Tetrahedron* **1998**, *54*, 13547−13556. (g) Yang, X.; Sugiyama, H.; Ikeda, S.; Saito, I.; Wang, A. H.-J. *Biophys. J.* **1998**, *75*, 1163−1171. (h) He, X.; Krawczyk, S. H.; Swaminathan, S.; Shea, R. G.; Dougherty, J. P.; Terhorst, T.; Law, V. S.; Griffin, L. C.; Coutre, S.; Bischofberger, N. *J. Med. Chem.* **1998**, *41*, 2234−2242. (i) Sherer, E. C.; Harris, S. A.; Soliva, R.; Orozco, M.; Laughton, C. A. *J. Am. Chem. Soc.* **1999**, *121*, 5981−5991. (j) Wang, Z.; Rizzo, C. J. *Org. Lett.* **2000**, *2*, 227−230. (k) Sugiyama, T.; Schweinberger, E.; Kazimierczuk, Z.; Ranmzaeva, N.; Rosemeyer, H.; Seela, F. *Chem. Eur. J.* **2000**, *6*, 369−378. (l) Sessler, J. L.; Sathiosatham, M.; Doerr, K.; Lynch, V.; Abboud, K. A. *Angew. Chem., Int. Ed.* **2000**, *39*, 1300−1303. (m) Seela, F.; Debelak, H. *Nucleic Acids Res.* **2000**, *28*, 3224−3232. (n) Wilhelmsson, L. M.; Holmen, A.; Lincoln, P.; Nielsen, P. E.; Norden, B. *J. Am. Chem. Soc.* **2001**, *123*, 2434−2435.
(4) For examples: (a) Sanghvi, Y. S. In *Antisense Research and Applications*; Crooke, S. T., and Lebleu, B., Eds.; CRC Press: Boca Raton, 1993; Ch. 15, pp 273−288. (b) Miller, P. S. In *Bioorganic Chemistry: Nucleic Acids*; Hecht, S. M., Ed.; Oxford University Press: Oxford, 1996; Ch. 12, pp 347−374. (c) Doronina, S. O.; Behr, J.-P. *Chem. Soc. Rev.* **1997**, *26*, 63−71. (d) Haginoya, N.; Ono, A.; Nomura, Y.; Ueno, Y.; Matsuda, A. *Bioconjugate Chem.* **1997**, *8*, 271−280. (e) Doronina, S. O.; Behr, J.-P. *Tetrahedron Lett.* **1998**, *39*, 547−550. (f) Heystek, L. E.; Zhou, H.; Dande, P.; Gold, B. *J. Am. Chem. Soc.* **1998**, *120*, 12165−12166. (g) Lin, K.; Matteucci, M. D. *J. Am. Chem. Soc.* **1998**, *120*, 8531−8532.
(5) Voegel, J. J.; Benner, S. A. *Helv. Chim. Acta* **1996**, *79*, 1881−1898.
(6) (a) Switzer, C.; Moroney, S. E.; Benner, S. A. *J. Am. Chem. Soc.* **1989**, *111*, 8322−8323. (b) Piccirilli, J. A.; Krauch, T.; Moroney, S. E.; Benner, S. A. *Nature* **1990**, 343, 33−37. (c) Roberts, C.; Bandaru, R.; Switzer, C. *J. Am. Chem. Soc.* **1997**, *119*, 4640−4649.
(7) (a) Ogawa, A. K.; Wu, Y.; McMinn, D. L.; Liu, J.; Schultz, P. G.; Romesberg, F. E. *J. Am. Chem. Soc.* **2000**, *122*, 3274−3287. (b) Wu, Y.; Ogawa, A. K.; Berger, M.; McMinn, D. L.; Schultz, P. G.; Romesberg, F. E. *J. Am. Chem. Soc.* **2000**, *122*, 7621−7632. (c) Ogawa, A. K.; Wu, Y.; Berger, M.; Schultz, P. G.; Romesberg, F. E. *J. Am. Chem. Soc.* **2000**, *122*, 8803−8804.
(8) Roberts, C.; Bandaru, R.; Switzer, C. *Tetrahedron Lett.* **1995**, *36*, 3601−3604.
(9) For the sake of simplicity, the aglycon of **1** (and **11**) shall be subsequently referred to as diamino. Similarly, those of **2**, **3**, and **4** (and each of the protected derivatives) shall be referred to as dioxo, amino-oxo, and oxo-amino, respectively. When these nucleoside units were incorporated into ODNs, the imidazopyridopyrimidine bases shall be referred to as $\mathbf{N^N}$, $\mathbf{O^O}$, $\mathbf{N^O}$, and $\mathbf{O^N}$, respectively.
(10) (a) Leonard, N. J.; Hiremath, S. P. *Tetrahedron* **1986**, *42*, 1917−1961. (b) Baus, A. K.; Niedernhofer, L. J.; Essigmann, J. M. *Biochemistry* **1987**, *26*, 5626−5635. (c) Lin, K.; Jones, R. J.; Matteucci, M. *J. Am. Chem. Soc.* **1995**, *117*, 3873−3874. (d) Godde, F.; Toulme, J.-J.; Moreau, S. *Nucleic Acids Res.* **2000**, *28*, 2977−2985. (e) Hirao, I.; Ohtsuki, T.; Fujiwara, T.; Mitsui, T.; Yokogawa, T.; Okuni, T.; Nakayama, H.; Takio, K.; Yabuki, T.; Kigawa, T.; Kodama, K.; Yokogawa, T.; Nishikawa, K.; Yokoyama, S. *Nature Biotech.* **2002**, *20*, 177−182.
(11) Gukian, K. M.; Schweitzer, B. A.; Ren, R. X.-F.; Sheils, C. J.; Tahmassebi, D. C.; Kool, E. T. *J. Am. Chem. Soc.* **2000**, *122*, 2213−2222.

Scheme 2 [a]

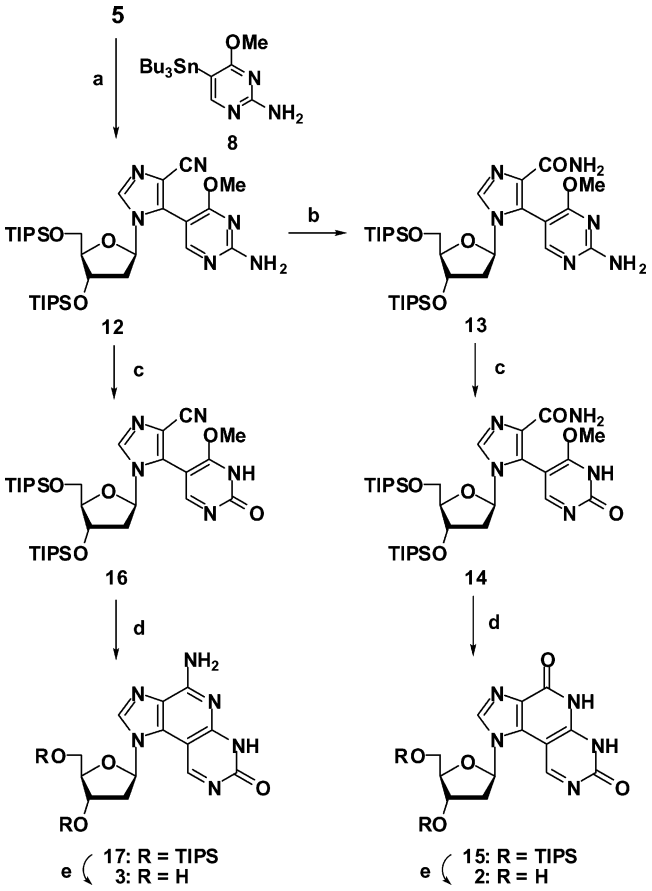

[a] Reagents: (a) $dba_3Pd_2{\cdot}CHCl_3$, DMF, 100 °C; (b) H_2O_2, NH_4OH-MeOH; (c) isoamyl nitrite, THF(aq), 60 °C; (d) NH_3/MeOH, 120 °C; and (e) TBAF, THF.

Scheme 3 [a]

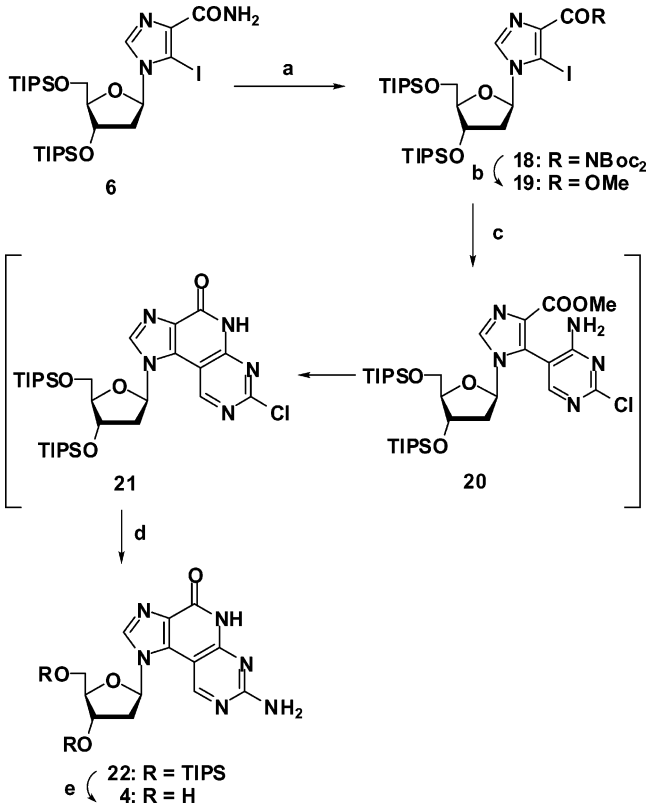

[a] Reagents: (a) $(Boc)_2O$, Et_3N, DMAP, CH_2Cl_2; (b) NaOMe, MeOH; (c) **7**, $dba_3Pd_2{\cdot}CHCl_3$, DMF, 100 °C; (d) 1,4-dioxane-NH_4OH, 100 °C; and (e) TBAF, THF.

First, the synthesis of the diamino derivative **1** was done by the reaction of **5** and **7** (Scheme 1). When a mixture of **5** and **7** was heated in DMF in the presence of tris(dibenzylideneacetone)dipalladium(0)-chloroform adduct ($dba_3Pd_2{\cdot}CHCl_3$), two fluorescent spots were detected by TLC analysis. The UV spectra of both spots showed absorption maxima at around 340 nm;[15] thus, the new spots were presumed to be the coupling products between **5** and **7**. In addition, the less polar spot on TLC was converted to the more polar spot when the reaction mixture was treated under basic conditions (see Experimental Procedures). As a result, the less polar spot was thought to be the coupling product **9** (not isolated), and spontaneous cyclization giving a tricyclic product **10** took place partially during the Stille coupling reaction. Treatment of **10** with a mixture of 1,4-dioxane and NH_4OH gave the diamino derivative **11** in 86% yield. Deprotection of the silyl groups with tetrabutylammonium fluoride (TBAF) gave the free nucleoside **1**.

Preparation of the dioxo derivative **2** and the amino-oxo derivative **3** was achieved via the Stille coupling reaction between **5** and **8**, as shown in Scheme 2. When a mixture of **5** and **8** was heated with $dba_3Pd_2{\cdot}CHCl_3$, **12** was obtained in 81% yield. To convert **12** into the dioxo derivative **2**, the 4-cyano group of **12** was hydrolyzed with hydrogen peroxide in the presence of NH_4OH to give the 4-carboxamide derivative **13** in 92% yield. Although **13** was observed as a single spot by TLC analysis, the ^1H NMR spectrum of **13** was somewhat complicated. For example, four sets of aromatic proton signals were observed at 8.17, 8.05, 7.87, and 7.86 ppm each as a singlet (in a ratio of 2:1:1:2) in $CDCl_3$. Interestingly, when the ^1H NMR measurement of **13** was carried out at 60 °C, the four sets of proton signals converged into two sets of proton signals at 8.12 and 7.81 ppm in a ratio of 1:1. Other proton signals were also simplified under the same conditions. Consequently, compound **13** is considered to exist as a mixture of rotamers, arising from steric repulsion between the spatially close amide and the methoxy substituents. Hydrolytic deamination of **13** by treatment with isoamyl nitrite in THF containing a small amount of H_2O gave **14** in 51% yield.[16] The existence of rotamers was also observed in the ^1H NMR spectrum of **14**. When the resulting **14** was heated with methanolic ammonia in a steel container, the dioxo derivative **15** was obtained in 73% yield. The amino-oxo derivative **17** was synthesized also starting from **12** using

(12) (a) Minakawa, N.; Sasabuchi, Y.; Kiyosue, A.; Kojima, N.; Matsuda, A. *Chem. Pharm. Bull*. **1996**, *44*, 288−295. (b) Napoli, L. D.; Messere, A.; Montesarchio, D.; Piccialli, G.; Varra, M. *J. Chem. Soc., Perkin Trans. 1* **1997**, 2079−2082.

(13) 2,4-Diaminopyrimidine and 2,4-dimethoxypyrimidine were also examined as starting materials to prepare the tributylstannylpyrimidine derivatives. In the former case, introduction of the tributylstannyl group did not work well, while in the latter, it was very difficult to carry out the intramolecular cyclization to give the desired tricyclic skeletons after the Stille coupling reaction.

(14) Additional references for the synthesis of **5**−**8**: (a) Minakawa, N.; Takeda, T.; Sasaki, T.; Matsuda, A.; Ueda, T. *J. Med. Chem*. **1991**, *34*, 778−786. (b) Harris, M. G.; Stewart, R. *Can. J. Chem*. **1977**, *55*, 3800−3806. (c) Das, B.; Kundu, N. G. *Synthetic Commun*. **1988**, *18*, 855−867.

(15) The maximal absorption of **5** was observed at 237 nm, while those of **7** were observed at 244 and 280 nm, respectively.

(16) This reaction was a modification of reductive deamination reported by Nair and Chamberlain, see Nair, V.; Chamberlain, S. D. *Synthesis* **1984**, 401−403.

the same procedure, that is, hydrolytic deamination, followed by the intramolecular cyclization. Both of the protected nucleosides **15** and **17** were deprotected with TBAF to give the free nucleosides **2** and **3**, respectively.

The synthesis of the remaining oxo-amino derivative **4** was next carried out, which was rather troublesome relative to those of the other tricyclic nucleosides **1**−**3**. The desired **22** is presumed to be obtained via the intramolecular cyclization of **13**, using the same method as for **15**. However, when **13** was treated with methanolic ammonia at 120 °C for 48 h in a steel container, the desired product **22** was not obtained, and **13** was recovered in quantitative yield. As compared with the intramolecular cyclization of **14**, that of **13** would be more difficult because of higher electron density of the pyrimidine moiety.[17] After several attempts, **22** was obtained efficiently as illustrated in Scheme 3. First, the 4-carboxamide group of **6** was converted to the methyl ester according to our previous method.[18] Thus, treatment of **6** with di-*tert*-butyl dicarbonate in the presence of Et_3N and DMAP gave **18** in 95% yield, which was then treated with NaOMe in MeOH to give **19** in 98% yield. After the Stille coupling reaction of **19** with **7** in the presence of $dba_3Pd_2{\cdot}CHCl_3$, the resulting crude brown syrup (probably including the intermediates **20** and **21**) was treated with a mixture of NH_4OH and 1,4-dioxane at 100 °C for 60 h in a steel container to give the oxo-amino derivative **22** in 57% yield in three steps. Deprotection of the silyl groups with TBAF gave the free nucleoside **4** in 81% yield.

2. Conformational Analysis Using NMR and NOE Experiments. The conformation of a nucleoside is critical for adopting a double helix structure when the nucleoside is incorporated into ODNs. Generally, a 2′-deoxyribonucleoside prefers a C2′-endo conformation of the sugar, which is also maintained in the B-DNA double helix structure.[19] Since the synthetic tricyclic nucleosides possess novel structures, conformational properties, such as the sugar pucker mode and the syn/anti equilibrium around the glycosyl bond, were first investigated on the nucleoside level. The sugar pucker mode of a nucleoside can be easily predicted from the ^{1}H NMR coupling constants of the ribose moiety.[20] The coupling constants ($J_{1',2'\beta}$ and $J_{3',4'}$) of **1**−**4** in DMSO-d_6 were determined. In **1**, the $J_{1',2'\beta}$ was determined as 6.0 Hz, while the $J_{3',4'}$ was 3.1 Hz; thus, the C2′-endo conformer was calculated to have a population of 66%. Similar values for both of the coupling constants were obtained in compounds **2**−**4** (see Experimental Procedures); thus, all of the novel tricyclic nucleosides prefer a C2′-endo conformation just as the natural deoxyribonucleosides (68% for **2**, 65% for **3**, and 64% for **4**).

The syn/anti equilibrium around the glycosyl bond was next examined using NOE experiments.[21] As is well-known, one can assume that if irradiation of H-8 in purine 2′-deoxyribonucleosides exhibits a strong NOE at H-1′ and small NOEs at H-2′β and H-3′, then the syn conformation is preferred. On the other hand, if irradiation of H-8 exhibits strong NOEs at H-2′β and H-3′ and a smaller NOE at H-1′, then the anti conformation is dominant. The NOE experiments were carried out using **4** by irradiation of H-2 (corresponding to the H-8 position of the purine base) and H-9 (the proton at the pyrimidine ring). Compound **4** exhibited a small NOE (1.3%) value at H-1′ and larger ones at H-2′β and H-3′ (5.6 and 2.3%) upon irradiation of H-2. In addition, a strong NOE (13.1%) was observed at H-1′ upon irradiation of H-9. The same NOE tendency was observed when the experiment was carried out at 80 °C (data not shown). As a result, **4** is thought to be a highly anti-constrained compound, which is also expected for **1**−**3**. In the DNA−DNA double helix, the nucleoside unit generally adopts the anti conformation to form the Watson−Crick H-bonding except for the unusual left-handed Z-DNA.[19] Consequently, it was concluded that the tricyclic nucleosides **1**−**4** would not structurally prevent double helix formation when these are incorporated into the ODNs.

3. Characterization of H-Bonding Motif Using ^{1}H NMR Spectroscopy. We designed the tricyclic nucleosides **1**−**4** with the aim of forming stable four H-bonds in synthetic ODNs. Since H-bonding interactions in monomers have provided considerable insight into those of the interior of polymeric units,[22] characterization of the H-bonding motifs of the tricyclic nucleosides was next investigated with ^{1}H NMR studies over a wide temperature range. The silylated derivatives (i.e., **11**, **15**, **17**, and **22**) were used for ^{1}H NMR measurements in the nonpolar solvent $CDCl_3$, and monitoring of the H-bonds was done to note downfield shifts of their amino and amide proton signals.[22,23]

As shown in Figure 1, the tricyclic nucleosides would form a heterodimer with four H-bonds between the diamino **11** and the dioxo **15** derivatives and the amino-oxo **17** and the oxo-amino **22** derivatives in a parallel direction. In addition to the heterodimer formation, **17** and **22** are both expected to form a homodimer with four H-bonds in an antiparallel direction as shown in Figure 2B. This type of interaction has already been observed in the NMR spectrum of **17**, measured at room temperature, that is, the amide proton at the 6 position was observed at 13.77 ppm, and the 4-amino protons were observed as distinct signals at 10.30 and 6.44 ppm (see Experimental Procedures). In contrast, the 4-amino protons were observed at 7.80 ppm as a single coalesced signal when the NMR spectrum of **17** was measured in DMSO-d_6 at room temperature. This result seemed to arise from an intermolecular interaction of **17** in $CDCl_3$. Consequently, the temperature-dependence studies were first carried out for the homodimers of **17** and **22**, respectively. As an example, the stacked partial ^{1}H NMR spectra of **22** at variable temperatures in $CDCl_3$ (at 25 mM) are shown in Figure 2A. No chemical shift changes of H-2, H-9, and H-1′ were observed between ±60 °C, while those of the amide and amino protons were dramatic. In the spectrum at 30 °C, the

(17) As in the case of **13**, treatment of **12** with methanolic ammonia did not give the diamino derivative **11**.

(18) Kojima, N.; Minakawa, N.; Matsuda, A. *Tetrahedron* **2000**, *56*, 7909−7914.
(19) Saenger, W. *Principles of Nucleic Acid Structure*; Springer-Verlag: New York, 1984; pp 253−282.
(20) For examples: (a) Altona, C.; Sundaralingam, M. *J. Am. Chem. Soc*. **1973**, *95*, 2333−2344. (b) Davies, D. B.; Danyluk, S. S. *Biochemistry* **1974**, *13*, 4417−4434.
(21) For examples: (a) Hart, P. A.; Davis, J. P. *J. Am. Chem. Soc*. **1969**, *91*, 512−513. (b) Davis, J. P.; Hart, P. A. *Tetrahedron* **1972**, *28*, 2883−2891. (c) Rosemeyer, H.; Toth, G.; Golankiewicz, B.; Kazimierczuk, Z.; Bourgeois, W.; Kretschmer, U.; Muth, H. P.; Seela, F. *J. Org. Chem*. **1990**, *55*, 5784−5790. (d) Minakawa, N.; Kojima, N.; Matsuda, A. *Heterocycles* **1996**, *42*, 149−154. (e) Minakawa, N.; Kojima, N.; Matsuda, A. *J. Org. Chem*. **1999**, *64*, 7158−7172.
(22) For examples: (a) Katz, L.; Penman, S. *J. Mol. Biol*. **1966**, *15*, 220−231. (b) Shoup, R. R.; Miles, H. T.; Becker, E. D. *Biochem. Biophys. Res. Commun*. **1966**, *23*, 194−201. (c) Newmark, R. A.; Cantor, C. R. *J. Am. Chem. Soc*. **1968**, *90*, 5010−5017.
(23) For examples: (a) Williams, L. D.; Shaw, B. R. *Proc. Natl. Acad. Sci. U.S.A.* **1987**, *84*, 1779−1783. (b) Williams, N. G.; Williams, L. D.; Shaw, B. R. *J. Am. Chem. Soc*. **1989**, *111*, 7205−7209. (c) Williams, L. D.; Williams, N. G.; Shaw, B. R. *J. Am. Chem. Soc*. **1990**, *112*, 829−833. (d) Sessler, J. L.; Wang, R. *J. Org. Chem*. **1998**, *63*, 4079−4091.

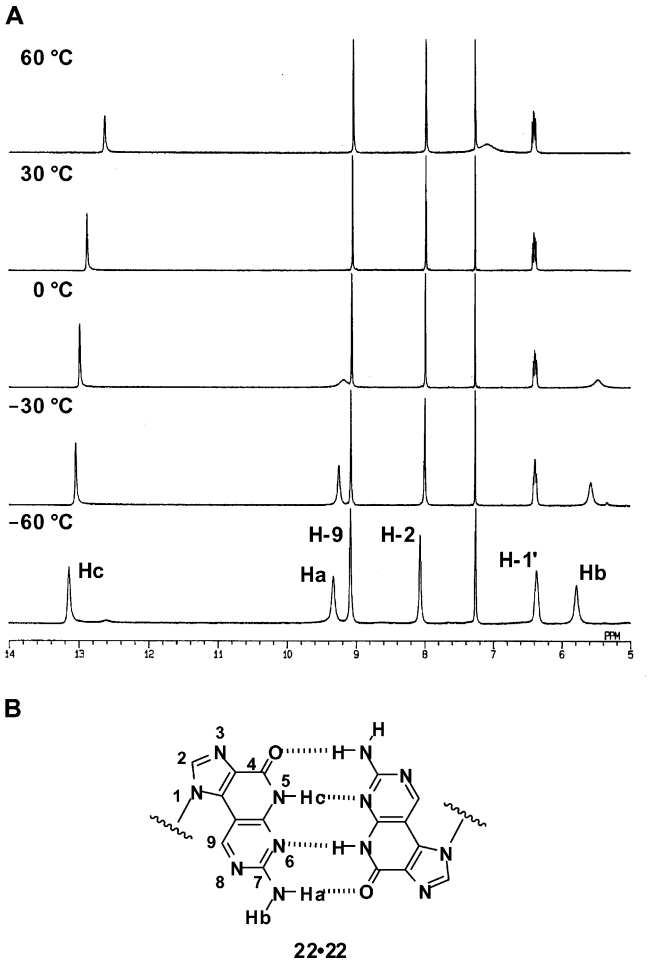

Figure 2. (A) Partial ^{1}H NMR spectra obtained in the course of carrying out a temperature-dependence study of **22** (270 MHz, 25 mM in $CDCl_3$). (B) Proposed aglycon structure of homodimer (**22·22**).

5-amide proton (Hc) was observed at 12.88 ppm, while the amino protons at the 7 position were not detected. When the measurement was done at 60 °C, the amide proton signal was shifted upfield, and the amino protons were observed at 7.16 ppm as a single coalesced signal. These results show that **22** prefers to exist as a monomer at that temperature. On the other hand, the amide proton signal was shifted downfield with decreasing temperatures. In addition, the amino protons were split into two sets of broad singlets, clearly observed at 9.33 ppm (Ha) and 5.79 ppm (Hb) at −60 °C in the spectrum. Therefore, the proton signals at 13.14 and 9.33 ppm would be involved in H-bonding, while that at 5.79 ppm is not involved in the H-bonding. On the basis of these results, **22** is considered to form the homodimer **22·22** in an antiparallel direction with four H-bonds at low temperature as illustrated in Figure 2B. This consideration was further confirmed by NOE experiments at −60 °C. Thus, a strong NOE (40.4%) was observed at the H-bonded amino proton (Ha) upon irradiation of the amide proton (Hc).

Since the resulting homodimer **22·22** still has H-bonding abilities on its N-3 and O-4 positions as a proton acceptor and the 7-amino group (Hb) as a proton donor, formation of more intricate H-bonded complexes such as tetramers may be possible. However, this is unlikely at least above −60 °C. This being the case, the Hb of **22** would also be involved in the H-bonding; thus, the Hb signal is expected to move downfield, depending on temperature.[23b] As can be seen in the spectra at 0, −30, and −60 °C, no significant downfield shift was observed in the frequency of the Hb signal (less than 0.4 ppm). Therefore, the equilibrium predominance between the monomer **22** and the homodimer **22·22** with four H-bonds was demonstrated, and formation of the more intricate H-bonded complexes was excluded in the temperature range from +60 to −60 °C. A similar phenomenon was also observed with **17** showing formation of a homodimer (Supporting Information).

To determine the heterodimer formation between **17** and **22**, ^{1}H NMR measurements were carried out by mixing 1 equiv of **17** (25 mM) with 1 equiv of **22** (25 mM) in $CDCl_3$. At 60 °C, two sets of amide protons were observed at 13.41 and 12.91 ppm, respectively, thus indicating that **17** and **22** seem to exist as monomers at that temperature. As the temperature was decreased, the spectra became complicated; two sets of additional amide protons were observed around 13.5 ppm at −30 °C. In addition, broad singlets assignable to the amino protons appeared. Such complicated spectra seem to be the result of formation of both homodimers (**17·17** and **22·22**) and the heterodimer (**17·22**). At −60 °C, the spectrum became clear, that is, four sets of amide protons ranging from 13.0 to 14.0 ppm and at least seven signals of the amino protons from 5.5 to 10.5 ppm were observed (Supporting Information). Proton signals of the heterodimer **17·22** could be assigned by comparison with those of the homodimers **17·17** and **22·22** at the same temperature. In Figure 3, the ^{1}H NMR spectrum of **17·22** at −60 °C is shown along with those of the homodimers. As a result, the proton signals, except for those of the homodimers, were easily detected. The proton signals indicated by arrows would correspond to a new structure formed at low temperature, and these are assigned to the aglycon protons of the heterodimer (**17·22**) with four H-bonds. Thus, the proton signals at 13.58 and 13.37 ppm are likely to be two sets of amide protons. The amino protons involved in H-bonding can be seen at 10.24 and 9.49 ppm, while those at 6.78 and 5.68 ppm are assigned as non-H-bonded amino protons. In addition, four aromatic protons were also detected between 9.3 and 8.0 ppm. Unfortunately, the H-bonding motif could not be confirmed by NOE experiments because each signal was too close to irradiate selectively. However, integral values of the signals corresponding to the heterodimer were essentially the same as those of the homodimers. Therefore, this also appears to support our findings that the heterodimer **17·22**, like the homodimers, consists of four H-bonds, as expected.

In contrast to the experiments using **17** and **22**, no obvious interaction between **11** and **15** was detected in the temperature-dependence studies. Neither amide nor amino proton signals were observed at 30 °C. These proton signals were still undetectable, except for one broad signal at 7.06 ppm, at 60 °C. Although several broad signals were observed when the temperature decreased, the spectrum was too complicated and broad to assign them (Supporting Information). However, **11** and **15** were thought to interact with each other through H-bonding because the insoluble dioxo derivative **15** in $CDCl_3$ was clearly dissolved upon addition of an equimolar amount of **11**. In addition, this type of interaction was suggested to occur even at 60 °C. In Figure 4, two partial spectra of the mixed sample (**11**:**15** = 1:1) and **11** at 60 °C are shown. Two sets of the amino proton signals were observed at 5.90 and 5.12 ppm,

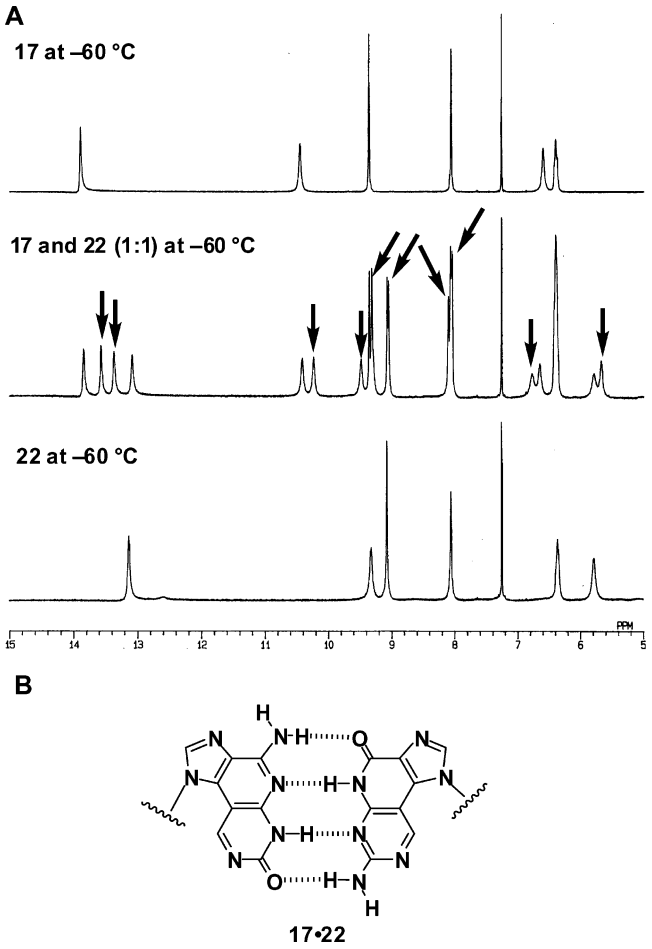

Figure 3. (A) Partial ^{1}H NMR spectra of **17** (top), **22** (bottom), and 1:1 mixtures of **17** and **22** (middle) at −60 °C (270 MHz, 25 mM in $CDCl_3$). (B) Proposed aglycon structure of heterodimer (**17**·**22**).

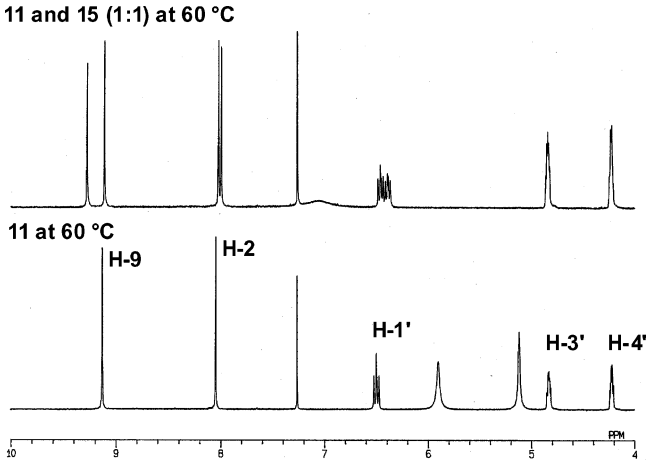

Figure 4. (A) Partial ^{1}H NMR spectra of 1:1 mixtures of **11** and **15** (top) and **11** (bottom) at 60 °C (270 MHz, 10 mM in $CDCl_3$).

each with an integral of two, in the spectrum of the diamino nucleoside **11**. On the other hand, a broad signal was observed at 7.06 ppm instead of these amino proton signals in that of the mixed sample. Although there is no direct evidence for the heterodimer formation between **11** and **15** consisting of four H-bonds, interactions between **11** and **15** through H-bonding are indicated by the above results. Unlike **17** and **22**, formation of stable homodimers are unlikely for both **11** and **15**. However, two sets of base pairing motifs with four H-bonds, namely, the parallel and antiparallel type, would be expected between them. In addition, formation of some other complexes (i.e., tetramer, oligomer, etc.) might occur in the monomers. These interactions may have caused the complicated spectra.

As is demonstrated, the tricyclic nucleosides **17** and **22** formed base pairs with four H-bonds. In contrast, no obvious evidence of base pairing with four H-bonds was obtained between **11** and **15** in monomers. However, the geometry and direction of the base pairing should be controllable when these nucleosides are introduced into ODNs. Therefore, further investigation of dioxo and diamino base pairing in polymers would be worth evaluating. The base pairing abilities of the tricyclic nucleosides in ODNs including comparison with natural Watson−Crick base pairing was next examined.

4. Synthesis of Oligodeoxynucleotides. After conversion of **1**−**4** into the corresponding phosphoramidites with appropriate protecting groups on each nucleobase (Supporting Information),[24] ODNs were synthesized on a DNA/RNA synthesizer by the phosphoramidite method.[25] Two sets of complementary 17mers (ODN I and II and ODN III and IV) were designed to investigate the H-bonding abilities of the tricyclic nucleosides, where the $\mathbf{N^N}$, $\mathbf{O^O}$, $\mathbf{N^O}$, and $\mathbf{O^N}$ were incorporated in the X and Y positions (see the sequences in Figures 5, 6, and 8). The fully protected ODNs (1 μmol) linked to the solid support were treated with concentrated NH_4OH at 55 °C for 16 h, followed by C-18 column chromatography. The ODNs were detritylated with 80% aqueous AcOH, and each ODN obtained showed a single peak on reverse-phase HPLC. Each ODN was completely hydrolyzed to the corresponding nucleosides by a mixture of nuclease P1, snake venom phosphodiesterase, and alkaline phosphatese, and the nucleoside composition was analyzed by HPLC. The peak corresponding to the tricyclic nucleosides $\mathbf{N^N}$, $\mathbf{O^O}$, $\mathbf{N^O}$, or $\mathbf{O^N}$, confirmed by coelution with authentic samples, was clearly observed, and the nucleoside composition calculated from the areas of the peaks supported the structure of each (Supporting Information).

5. Thermal Stability of the DNA−DNA Duplexes Containing Base Pairings between Imidazopyridopyrimidine Bases. Thermal stability of duplexes formed by ODN I and complementary ODN II, which contained one molecule of the $\mathbf{N^N}$, $\mathbf{O^O}$, $\mathbf{N^O}$, or $\mathbf{O^N}$ in their X or Y position, was first studied by thermal denaturation in a buffer of 0.01 M sodium cacodylate (pH 7.0) containing 0.1 M NaCl. Each profile of the thermal denaturation showed a single transition corresponding to a helix-to-coil transition to give melting temperatures (T_m). The thermodynamic parameters ($\Delta H°$, $\Delta S°$, and $\Delta G°$) of the duplexes were determined by calculations based on the slope of a $1/T_m$ versus $\ln(C_T/4)$ plot,[26] where C_T is total concentration of single strands (Supporting Information). The melting temperature (T_m) values represented by bar graph and negative free energy ($-\Delta G°_{298}$) are shown in Figure 5. Differences in the T_m values of the duplexes containing the tricyclic nucleosides were quite small (5.6 °C; maximum, 59.6 °C; minimum, 54.0 °C), and no

(24) References for the synthesis of phosphoramidites: (a) Kamaike, K.; Hasegawa, Y.; Ishido, Y. *Nucleosides Nucleotides* **1988**, *7*, 37−43. (b) Froehler, B. C.; Matteucci, M. D. *Nucleic Acids Res.* **1983**, *11*, 8031−8036. (c) Caruthers, M. H.; McBride, L. J.; Bracco, L. P.; Dubendorff, J. W. *Nucleosides Nucleotides* **1985**, *4*, 95−105.
(25) Sinha, N. D.; Biernat, J.; Koster, H. *Tetrahedron Lett.* **1983**, *24*, 5843−5846.
(26) Breslauer, K. J. In *Methods in Molecular Biology, Volume 26, Protocols for Oligonucleotide Conjugates*; Agrawal, S., Ed.; Humana Press Inc.: Totowa, New Jersey, 1994; Ch. 14, pp 347−372.

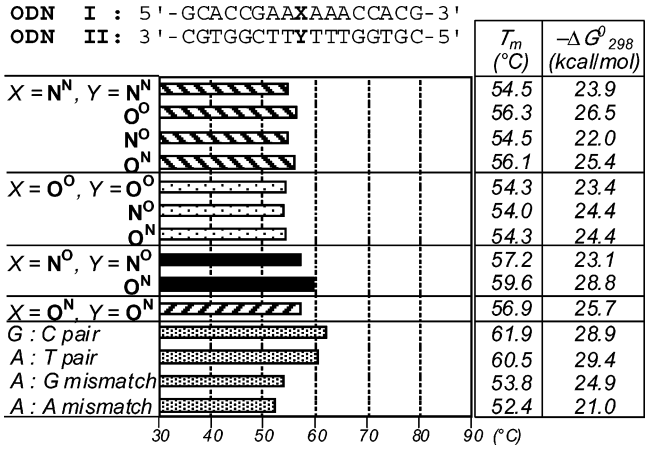

Figure 5. Hybridization data of ODNs I:II (X and Y = $\mathbf{N^N}$, $\mathbf{O^O}$, $\mathbf{N^O}$, or $\mathbf{O^N}$). Experimental conditions are described in Experimental Procedures.

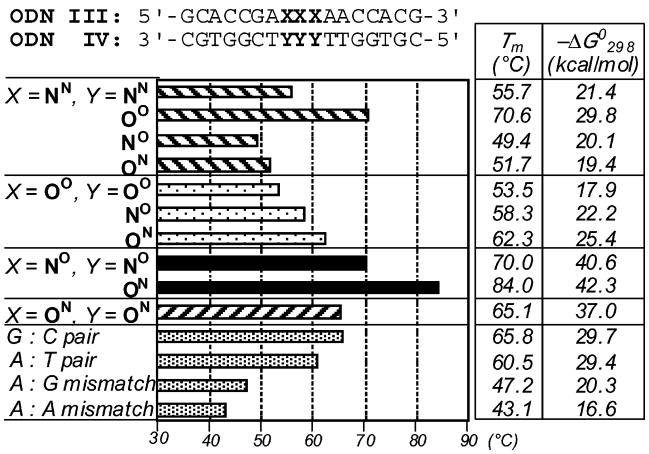

Figure 6. Hybridization data of ODNs III:IV (X and Y = $\mathbf{N^N}$, $\mathbf{O^O}$, $\mathbf{N^O}$, or $\mathbf{O^N}$). Experimental conditions are described in Experimental Procedures.

apparent specificity of base pairing was observed. Although the duplex with the $\mathbf{N^O}$:$\mathbf{O^N}$ pair had the highest T_m value (59.6 °C), this value was lower than not only that of the duplex with the G:C pair (T_m = 61.9 °C) but also that with the A:T pair (T_m = 60.5 °C). Thus, contrary to our expectation, when one molecule of the tricyclic nucleosides was incorporated into each strand, the thermal and thermodynamic stabilities of the duplexes did not increase. The T_m values of the duplexes formed by ODN I and II were all slightly lower than those of the duplexes containing a natural G:C or A:T pair at the corresponding positions.

On the other hand, when three molecules of the tricyclic nucleosides were consecutively incorporated into the center of each ODN (ODNs III and IV), the thermal and thermodynamic stabilization of the duplexes due to the specific base pairings was observed. As shown in Figure 6, the best result was obtained in the case of the duplex containing the $\mathbf{N^O}$:$\mathbf{O^N}$ pair (T_m = 84.0 °C). The value was between 18.2 and 23.5 °C higher than those of the duplexes containing three consecutive G:C (T_m = 65.8 °C) and A:T pairs (T_m = 60.5 °C), respectively. Consequently, it was found that the $\mathbf{N^O}$:$\mathbf{O^N}$ pair stabilized the duplex by about +6 and +8 °C per modification as compared with those of the duplexes containing the G:C and A:T pairs, respectively. As described in section 3, no obvious H-bonding motif was observed between $\mathbf{N^N}$ and $\mathbf{O^O}$ in the monomers. In this experiment, however, the $\mathbf{N^N}$:$\mathbf{O^O}$ pair showed a rather higher

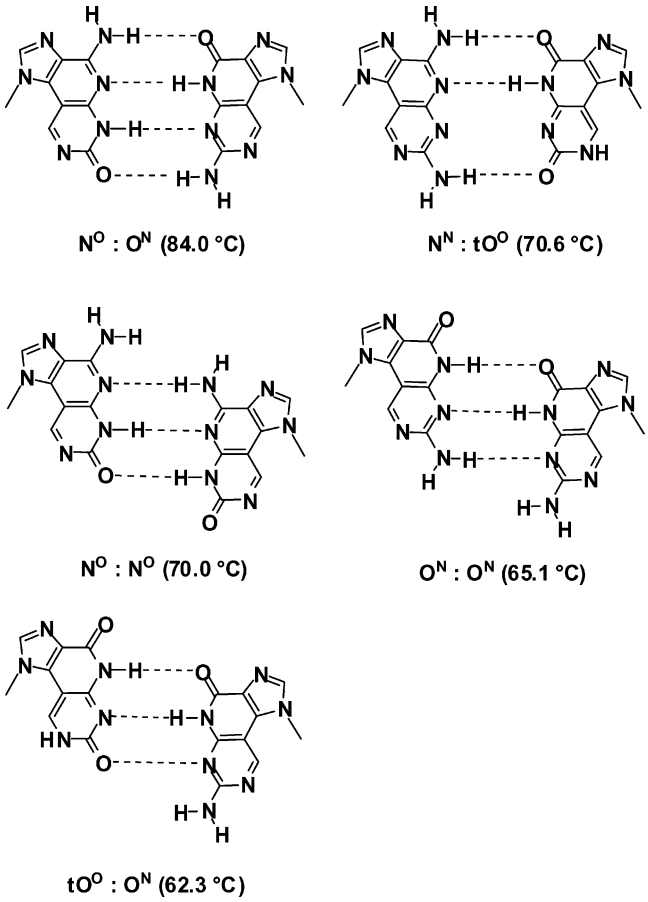

Figure 7. Possible base pairing motifs between imidazopyridopyrimidine bases.

T_m of 70.6 °C. The duplex containing the $\mathbf{N^O}$:$\mathbf{N^O}$ pairs (T_m = 70.0 °C) was also stabilized to the same degree as that of the $\mathbf{N^N}$:$\mathbf{O^O}$ pairs. These T_m values are distinctly lower than that of the $\mathbf{N^O}$:$\mathbf{O^N}$ pair and rather close to the G:C pair. Consequently, we propose their possible base pairing motifs to be those shown in Figure 7. As is supported in the temperature dependent NMR study, $\mathbf{N^O}$ and $\mathbf{O^N}$ can form base pairs with four H-bonds even when they are incorporated into ODNs to give the thermally and thermodynamically stable duplex. In the case of the $\mathbf{N^N}$:$\mathbf{O^O}$ pair, a reasonable explanation for the above result would be that this base pair has fewer H-bonds than the expected four (Figure 1). A tautomeric form of $\mathbf{O^O}$, represented as $\mathbf{tO^O}$, can be considered, and this could form a base pair with $\mathbf{N^N}$ by three H-bonds, as shown in Figure 7 ($\mathbf{N^N}$:$\mathbf{tO^O}$). The T_m value of the duplex containing the $\mathbf{N^O}$:$\mathbf{N^O}$ pair predicts that this pair also has three H-bonds. These T_m values are in good agreement with those of the G:C pair, which has three H-bonds, implying that the proposed base pairing motifs are reasonable. Except for these three pairs, the $\mathbf{O^N}$:$\mathbf{O^N}$ and $\mathbf{O^O}$:$\mathbf{O^N}$ (represented as $\mathbf{tO^O}$:$\mathbf{O^N}$ in Figure 7) pairs also stabilized the duplexes relative to the A:T pair, and the proposed motifs are illustrated. The remaining five combinations were less stable than the duplex containing the A:T pair; however, all of them were more stable than the duplexes containing the A:G and A:A mismatched pairs. Since the T_m of the duplex containing $\mathbf{N^O}$:$\mathbf{O^N}$ went up dramatically and the ΔT_m [T_m ($\mathbf{N^O}$:$\mathbf{O^N}$) − T_m ($\mathbf{N^N}$:$\mathbf{N^O}$)] was quite large (34.6 °C), it can be concluded that the H-bonding abilities between the imidazopyridopyrimidine bases are essential and affect the thermal stability of the duplex. The attached $-\Delta G°_{298}$ data also

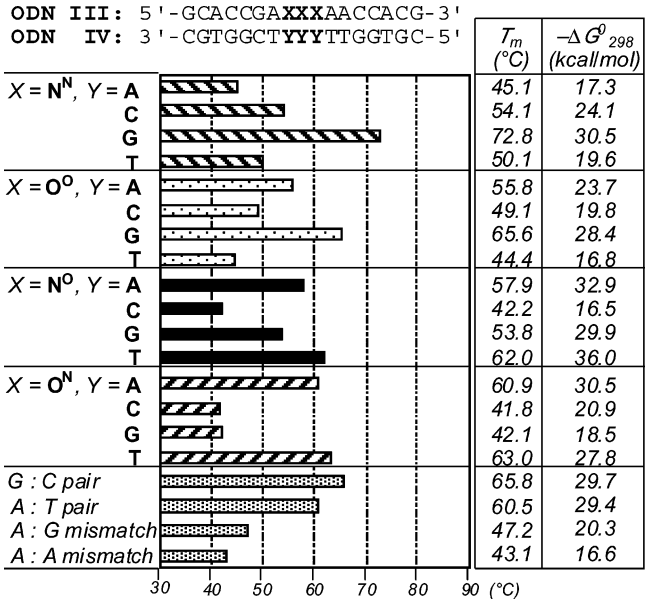

Figure 8. Hybridization data of ODNs III:IV (X = $\mathbf{N^N}$, $\mathbf{O^O}$, $\mathbf{N^O}$, or $\mathbf{O^N}$, Y = A, C, G, or T). Experimental conditions are described in Experimental Procedures.

support this conclusion. A stacking interaction influence, arising from the extended aromatic surface of the imidazopyridopyrimidine bases, may also contribute to their stabilities.[27,28] This will be discussed in section 7 of this paper.

6. Thermal Stability of the DNA−DNA Duplexes Containing Base Pairings between the Imidazopyridopyrimidine Bases and the Natural Bases. In the previous section, we showed that consecutive incorporation of $\mathbf{N^O}$:$\mathbf{O^N}$ pairs into the duplexes markedly enhanced the thermal and thermodynamic stability of the duplex by four H-bonds. Since the imidazopyridopyrimidine bases possess multiple types of H-bonding ability, formation of stable base pairs with a natural base was predicted. Thus, an investigation of base pairing with natural bases was next undertaken using ODNs I:II and III:IV, where $\mathbf{N^N}$, $\mathbf{O^O}$, $\mathbf{N^O}$, or $\mathbf{O^N}$ was introduced at the X position, and A, C, G, or T was introduced at the Y position. When ODNs I and II were used, as in the preceding results, no base pair was found more stable than the G:C pair (data not shown). In contrast, a striking change was observed in the investigations of ODNs III:IV. The T_m values represented by bar graph and negative free energy ($-\Delta G^\circ_{298}$) are shown in Figure 8. Among the 16 combinations, the duplex containing the $\mathbf{N^N}$:G pair, which had the highest T_m (72.8 °C), was stabilized by +7.0 °C relative to the duplex containing the G:C pair (+2.3 °C per modification). The $\mathbf{O^O}$ also preferred G to give a thermally stable duplex equal to the duplex containing the G:C pair (65.6 vs 65.8 °C), while $\mathbf{N^O}$ and $\mathbf{O^N}$ showed different preferences in base pairing. In the case of $\mathbf{N^O}$, the most stable pair was $\mathbf{N^O}$:T (T_m = 62.0 °C). The $\mathbf{O^N}$ preferred both A and T to give the T_m values of 60.9 °C ($\mathbf{O^N}$:A) and 63.0 °C ($\mathbf{O^N}$:T), respectively. Interestingly, no stable pair with C was observed. If the $\mathbf{O^O}$ took the form shown in Figure 1, this form should make a stable base pair with C. In fact, however, G was the best partner of $\mathbf{O^O}$ but not of C. These results strongly suggest that the tautomeric form $\mathbf{tO^O}$ is preferable, as discussed in the previous section. The possible base pairing motifs of the imidazopyridopyrimidine base with the natural bases, which had higher T_m values than the duplex containing A:T pair, are illustrated in Figure 9. Consequently, it was found that the imidazopyridopyrimidine base also forms base pairs with the natural bases with some sequence specificities.

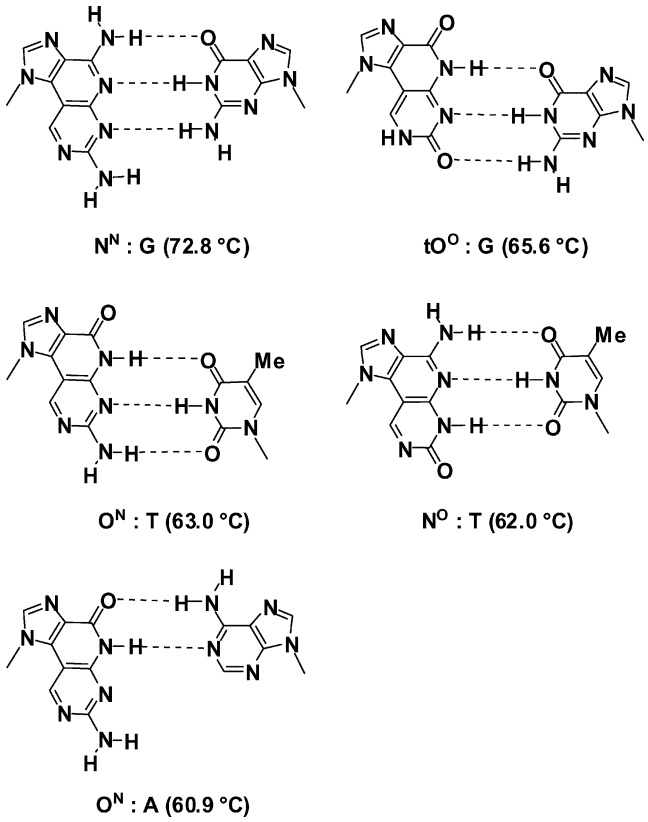

Figure 9. Possible base pairing motifs between imidazopyridopyrimidine base and natural base.

7. Measurement of Stacking Abilities of the Imidazopyridopyrimidine Bases. From the results described in sections 5 and 6, it was shown that the H-bonding abilities of the imidazopyridopyrimidine base are quite essential for the stability of the duplex. In this section, we discuss the effects of the stacking abilities of the imidazopyridopyrimidine bases. As mentioned above, these nucleobases have extended aromatic surfaces, and this would also contribute to the duplex stability.[27,28] For example, one can see stabilization of the duplex by the $\mathbf{N^N}$:G pair relative to the G:C pair, despite each pair being predicted to have the same number of H-bonds (Figure 9). This result undoubtedly implies that the stacking interaction would also be an important contributing factor for the stability. For this reason, evaluation of the stacking abilities was next examined. According to the method reported by Guckian et al.,[28] a series of duplexes, where Z was added at the end of each paired duplex (dangling end), were prepared, and the T_m values and the thermodynamic parameters of the duplexes were determined. Results of the thermodynamic parameters made in a buffer of 0.01 M sodium phosphate (pH 7.0) containing 1 M NaCl are presented in Table 1. As a comparison, the T_m data

(27) For examples: (a) Lin, K.-Y.; Jones, R. J.; Matteucci, M. *J. Am. Chem. Soc*. **1995**, *117*, 3873−3874. (b) Brotschi, C.; Haberli, A.; Leumann, C. J. *Angew. Chem., Int. Ed*. **2001**, *40*, 3012−3014. (c) Hashmi, S. A. N.; Hu, X.; Immoos, C. E.; Lee, S. J.; Grinstaff, M. W. *Org. Lett*. **2002**, *4*, 4571−4574.

(28) Guckian, K. M.; Schweitzer, B. A.; Ren, R. X.-F.; Sheils, C. J.; Paris, P. L.; Tahmassebi, D. C.; Kool, E. T. *J. Am. Chem. Soc*. **1996**, *118*, 8182−8183.

Table 1. Measurement of Aromatic Stacking Abilities

5′-Z/C G C G C G
G C G C G C/Z-5′

Z	T_m (°C)[a]	ΔT_m (°C)[b]	$-\Delta G°_{298}$[a] (kcal/mol)	$\Delta\Delta G°_{298}$[b]
none	42.7		10.4	
thymine (**T**)	47.3	4.6	11.4	1.0
cytosine (**C**)	47.5	4.8	11.7	1.3
adenine (**A**)	52.2	9.5	12.8	2.4
guanine (**G**)	52.4	9.7	12.9	2.5
$\mathbf{N^N}$	57.0	14.3	14.6	4.2
$\mathbf{O^O}$	52.5	9.8	12.8	2.4
$\mathbf{N^O}$	58.8	16.1	16.0	5.6
$\mathbf{O^N}$	57.4	14.7	14.2	3.8

[a] Experimental conditions are described in Experimental Procedures. [b] Stacking parameters (ΔT_m, $\Delta\Delta G°$) were obtained by subtracting data for the core hexamer duplex from that for duplexes possessing the unpaired (Z) unit.

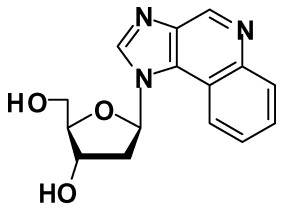

23 (IQ)

Figure 10. Structure of **IQ**.

for nondangling and natural bases (T, C, A, or G) at the dangling end are listed. The two unpaired Ts added +4.6 °C of T_m and +1.0 kcal/mol of $-\Delta G°_{298}$ relative to the self-complementary duplex (Z = none), and the Cs also added a similar stability. The unpaired purines (Z = A and G) afforded about 2-fold the duplex stability relative to the pyrimidines arising from expansion of the aromatic surface. These results agreed with those reported by Guckian et al. Among the tested compounds, $\mathbf{N^O}$ showed the highest T_m increase over the unsubstituted duplex of 16.1 °C (8.0 °C per base) and a total stacking energy of 5.6 kcal/mol (2.8 kcal/mol per base). The $\mathbf{N^N}$ and $\mathbf{O^N}$ also showed almost 1.5× higher stacking ability than those of the natural purines and 3× those of pyrimidines. Even though the efficacy of $\mathbf{O^O}$ was slightly low,[29] it was almost equal to those of adenine and guanine. From these results, it was revealed that the stacking abilities of the imidazopyridopyrimidine bases also increase the duplex stability, and this would be enhanced by three consecutive introductions of these bases into the ODNs.

To clarify whether the H-bonding ability or the stacking ability of the imidazopyridopyrimidine bases is the essential factor for the duplex stability, we prepared the imidazoquinoline derivative **23** (**IQ**; Figure 10).[30] Compound **23** was designed to eliminate the H-bonding ability except for one position but still have the same size of aromatic surface. Using this nucleoside unit, the T_m measurement of the duplex composed of ODNs III and IV, where **IQ** and $\mathbf{O^N}$ were introduced at the X and Y positions, respectively, was carried out. The duplex containing the **IQ**:$\mathbf{O^N}$ pair (T_m = 47.2 °C) was drastically destabilized by −36.8 °C relative to the duplex containing the $\mathbf{N^O}$:$\mathbf{O^N}$ pair (T_m = 84.0 °C; Figure 6). In contrast, the stacking ability of **IQ**, estimated by the T_m of the two unpaired **IQ** at the Z position (T_m = 61.5 °C), was higher than that of the $\mathbf{N^O}$ (T_m = 58.8 °C; Table 1). Consequently, in our substrates, it can be concluded that the H-bonding ability is the essential factor in the high duplex stability, for example, with the $\mathbf{N^O}$:$\mathbf{O^N}$ pair, and the stacking ability is a minor component of the stability.

Table 2. Sequences of ODNs and Hybridization Data of ODN V:VI−XII

		T_m (°C)[a]
ODN V	3′-CGTGGCTGGGTTGGTGC-5′	
ODN VI	5′-GCACCGACCCAACCACG-3′	68.3
ODN VII[b]	---------N^N---------	67.2
ODN VIII[b]	-------N^N-N^N-------	64.3
ODN IX[b]	---N^N----N^N----N^N---	63.0
ODN X[b]	-N^N--N^N--N^N----N^N--N^N-	55.7
ODN XI[b]	-------$N^N N^N N^N$-------	72.8
ODN XII[b]	-N^N-$N^N N^N$--$N^N N^N N^N$--$N^N N^N$-N^N-	75.7

[a] Experimental conditions are described in Experimental Procedures. [b] Sequences are same as ODN VI except for $\mathbf{N^N}$.

8. Why Consecutive Introduction of the Imidazopyridopyrimidine Bases Markedly Enhances the Thermal and Thermodynamic Stability of the Duplexes. As described above, introduction of one molecule of the imidazopyridopyrimidine base slightly destabilizes the duplex despite preferable base pairings such as $\mathbf{N^O}$:$\mathbf{O^N}$ and $\mathbf{N^N}$:G is introduced. In contrast, three consecutive introductions of these base pairs markedly stabilizes the duplexes. To elucidate these results, we further examined the sequence dependence of T_m using the duplexes containing the $\mathbf{N^N}$:G pair. Thus, setting the T_m of the duplex between ODNs V and VI as a control (68.3 °C), the sequence dependent variation was compared by substituting the G:C pair with the G:$\mathbf{N^N}$ pair at various positions (ODNs V:VII−XII). The sequences of ODNs and resulted T_m values are shown in Table 2. It was found that the duplexes became thermally less stable as the numbers of nonconsecutive isolated introductions of the G:$\mathbf{N^N}$ pairs increased (ODNs VII−X). On the other hand, the duplexes containing the consecutive G:$\mathbf{N^N}$ pairs were more stable than the control duplexes (ODNs XI and XII). Through comparison of the results between ODNs V:IX (T_m = 63.0 °C) and V:XI (T_m = 72.8 °C), it was revealed that consecutive introductions of a preferable base pairing motif is essential in contributing to the thermal stability of the duplex.

We considered these results, and the hypothetical structures are illustrated in Figure 11. The base pairs such as $\mathbf{N^O}$:$\mathbf{O^N}$ and $\mathbf{N^N}$:G form stable H-bonds in the duplex. However, the pairs would spread the width of the helix around the strand where they were introduced. Thus, it is known that the average intrastrand C1′−C1′ distance in a canonical Watson−Crick base pair is 10.5 (±0.2) Å, while the distances in purine(anti)−purine(anti) base pairs are typically much longer.[31] For example, Privé et al. reported the C1′−C1′ distance in the G(anti)−A(anti) mismatch to be 12.5 Å in an X-ray structure.[32] The intrastrand

(29) Although relationships between stacking abilities of the imidazopyridopyrimidine bases and their physical properties such as log *P*, dipole moment, and surface area were examined, no obvious result was obtained to explain the low stacking ability of $\mathbf{O^O}$; see ref 11.
(30) The synthesis of **IQ** was done via the Stille coupling reaction of 1-(2-deoxy-3,5-di-*O*-triisopropylsilyl-*β*-D-ribofuranosyl)-5-iodoimidazole-4-carbonitrile with *N*-acetyl-2-tributylstannylaniline; see Supporting Information.
(31) Coté, M. L.; Georgiadis, M. M. *Acta Crystallogr*. **2001**, *D57*, 1238−1250.
(32) Privé, G. G.; Heinemann, U.; Chandrasegaran, S.; Kan, L.-S.; Kopka, M. L.; Dickerson, R. E. *Science* **1987**, *238*, 498−504.

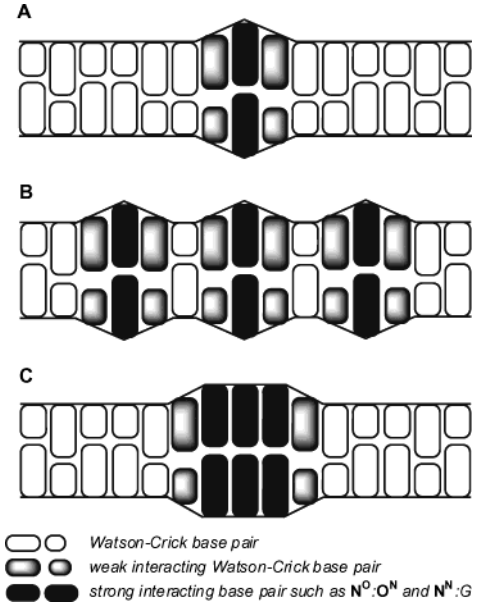

Figure 11. Hypothetical structures of our consideration.

C1′−C1′ distance in $\mathbf{N^O}$:$\mathbf{O^N}$ and $\mathbf{N^N}$:G would be similar to the above distance. Therefore, we speculated that thermal and thermodynamic destabilization of the duplex occurs at both sides of these pairs. When one pair of the tricyclic nucleoside was incorporated into the duplex, the destabilization factor arising from disruption of the Watson−Crick base pairs next to the pair would be greater than the stabilization arising from the stable H-bonds. Consequently, the duplex would become less stable (Figure 11A). This undesirable effect would be enhanced as the numbers of the nonconsecutive tricyclic nucleosides increased (Figure 11B). On the other hand, when the tricyclic nucleosides were consecutively incorporated into the duplex, the duplex would be thermally and thermodynamically stabilized to a great extent since the base pairs between the tricyclic nucleosides has stable H-bonds and a strong stacking ability with the adjacent bases. These stabilization factors would be superior to the conformational destabilization around the boundary of the base pairs (Figure 11C). To prove these considerations, an ODN, 5′-GCACCGT$\mathbf{N^O}\mathbf{N^O}\mathbf{N^O}$TACCACG-3′, was prepared, and a T_m with ODN IV (Y = $\mathbf{O^N}$), 3′-CGTGGC-T$\mathbf{O^N}\mathbf{O^N}\mathbf{O^N}$TTGGTGC-5′, which contains two T−T mismatches next to the tricyclic nucleosides, was measured. If the above considerations were correct, this duplex would show a similar T_m relative to the complementary duplex (ODNs III:IV; X = $\mathbf{N^O}$, Y = $\mathbf{O^N}$) because the H-bonding interaction of the base pair adjacent to the $\mathbf{N^O}$:$\mathbf{O^N}$ pair would be negligible. In fact, the T_m obtained from this duplex was 76.2 °C, which was 7.8 °C less stable than that of the complementary duplex (84.0 °C). However, the degree of destabilization of this duplex seems rather low despite the duplex containing the two T:T mismatches.[33] This result implied that the H-bonding interaction of the base pair adjacent to the favorable base pair such as $\mathbf{N^O}$:$\mathbf{O^N}$ and $\mathbf{N^N}$:G became weaker, thereby acting as a destabilizing factor in the duplex. It can be concluded that the thermal stability of the duplex would depend on a balance of stabilization and destabilization factors and that the duplex is markedly stabilized when the favorable base pairs were introduced consecutively into the duplex. Of course, our conclusion will not be applicable in all cases. In the case of an unfavorable base pair such as $\mathbf{N^N}$:$\mathbf{N^O}$, flip-out of either base from the duplex may minimize its destabilization.

In conclusion, the synthesis of four imidazo[5′,4′:4,5]pyrido-[2,3-*d*]pyrimidine nucleosides **1**−**4** has been accomplished via the Stille coupling of 5-iodoimidazole nucleosides with an appropriate 5-stannylpyrimidine derivative. Using ODNs containing these tricyclic nucleosides, preferable base pairing motifs were investigated. When ODNs containing one residue of the nucleoside were used, no base pairing motif was found to be more stable than either the G:C or the A:T pair. On the other hand, three consecutive introductions of the nucleosides were quite effective, and the $\mathbf{N^O}$:$\mathbf{O^N}$ pair markedly stabilized the duplex. The ΔT_m as compared with the G:C pair was +18.2 °C, and this pair stabilized the duplex by about +6 °C per modification. We presented the results that formation of four H-bonds of the $\mathbf{N^O}$:$\mathbf{O^N}$ pair and the stacking ability also contributed to the increased stabilization. We expected that the $\mathbf{N^O}$:$\mathbf{O^N}$ pair will find use in the stabilization and regulation of a variety of DNA structures depending on positions where it is incorporated. The use of the imidazopyridopyrimidine nucleosides in nucleic acid chemistry should be the focus of further study.

Experimental Procedures

General Methods. Physical data were measured as follows; melting points are uncorrected. ^{1}H and ^{13}C NMR spectra were recorded at 270, 400, or 500 MHz and 67.5, 100, or 125 MHz in $CDCl_3$ or DMSO-d_6 as the solvent with tetramethylsilane as an internal standard. Chemical shifts are reported in parts per million (δ), and signals are expressed as s (singlet), d (doublet), t (triplet), q (quartet), m (multiplet), or br (broad). All exchangeable protons were detected by addition of D_2O. Assignment of ^{1}H signals was based on two-dimensional NMR and NOE experiments. Mass spectra were measured on a JEOL JMS-D300 spectrometer. TLC was done on Merck Kieselgel F254 precoated plates. Silica gel used for column chromatography was Merck silica gel 5715.

4-Amino-7-chloro-1-(2-deoxy-3,5-di-*O*-triisopropylsilyl-*β*-D-ribofuranosyl)imidazo[5′,4′:4,5]pyrido[2,3-*d*]pyrimidine (10). To a mixture of **5** (2.20 g, 3.4 mmol) and **7** (2.13 g, 5.1 mmol) in DMF (25 mL) was added $dba_3Pd_2{\cdot}CHCl_3$ (280 mg, 0.27 mmol), and the whole mixture was heated at 100 °C for 11 h. The reaction mixture was filtered through a Celite pad and washed with AcOEt. The combined filtrate and washings were diluted with AcOEt and washed with H_2O (3×), followed by brine. The organic layer was dried (Na_2SO_4) and concentrated in vacuo to give a crude mixture of **9** and **10**. The resulting mixture was dissolved in a mixture of EtOH-5% aqueous Na_2CO_3, and the reaction mixture was heated at 80 °C for 1 h. The solvent was removed in vacuo, and the residue was partitioned between $CHCl_3$ and H_2O. The separated organic layer was washed with H_2O, followed by brine. The organic layer was dried (Na_2SO_4) and concentrated in vacuo. The residue was purified by a silica gel column and eluted with 0−5% EtOH in $CHCl_3$, to give **10** (1.53 g, 69%, crystallized from acetone-hexane): mp 262−264 °C; FAB-LRMS *m*/*z* 649 (MH^+); ^{1}H NMR ($CDCl_3$) δ: 9.36 (s, 1 H), 8.21 (s, 1 H), 6.60 (br s, 2 H), 6.52 (dd, 1 H, J = 7.8, 5.2 Hz), 4.83 (ddd, 1 H, J = 5.0, 2.7, 1.4 Hz), 4.24 (ddd, 1 H, J = 1.4, 2.8, 3.6 Hz), 3.88 (dd, 1 H, J = 2.8, 11.3 Hz), 3.84 (dd, 1 H, J = 3.6, 11.3 Hz), 2.71 (ddd, 1 H, J = 7.8, 12.5, 5.0 Hz), 2.65 (ddd, 1 H, J = 5.2, 12.5, 2.7 Hz), 1.11−0.98 (m, 42 H); ^{13}C NMR ($CDCl_3$) δ: 159.60, 159.05, 157.46, 153.91, 139.31, 131.75, 128.85, 107.06, 89.32, 86.30, 72.59, 63.28, 41.21, 18.02, 17.89, 12.12, 11.84. Anal. Calcd. for $C_{31}H_{53}ClN_6O_3Si_2$: C, 57.33; H, 8.23; N, 12.94. Found: C, 57.49; H, 8.31; N, 12.73.

(33) Insertion of one T:T mismatch in ODNs destabilized the duplex by −15 °C, see Peyret, N.; Seneviratne, A.; Allawi, H. T.; SantaLucia, J., Jr. *Biochemistry* **1999**, *38*, 3468−3477.

4,7-Diamino-1-(2-deoxy-3,5-di-*O*-triisopropylsilyl-β-D-ribofuranosyl)imidazo[5′,4′:4,5]pyrido[2,3-*d*]pyrimidine (11). To a solution of **10** (410 mg, 0.63 mmol) in 1,4-dioxane (20 mL) was added NH_4OH (28%, 20 mL), and the whole was heated at 100 °C for 24 h in a steel container. The solvent was removed in vacuo, and the residue was partitioned between $CHCl_3$ and H_2O. The separated organic layer was washed with H_2O, followed by brine. The organic layer was dried (Na_2SO_4) and concentrated in vacuo. The residue was purified by a silica gel column and eluted with 0−16% EtOH in $CHCl_3$, to give **11** (338 mg, 86%, crystallized from acetone): mp >270 °C (dec); FAB-LRMS *m*/*z* 630 (MH^+); ^{1}H NMR ($CDCl_3$) δ: 9.13 (s, 1 H), 8.06 (s, 1 H), 6.48 (dd, 1 H, *J* = 7.7, 5.3 Hz), 5.91 and 5.14 (each br s, each 2 H), 4.81 (ddd, 1 H, *J* = 5.0, 3.0, 1.6 Hz), 4.21 (ddd, 1 H, *J* = 1.6, 2.9, 3.8 Hz), 3.90 (dd, 1 H, *J* = 2.9, 11.2 Hz), 3.84 (dd, 1 H, *J* = 3.8, 11.2 Hz), 2.65 (ddd, 1 H, *J* = 7.7, 12.4, 5.0 Hz), 2.60 (ddd, 1 H, *J* = 5.3, 12.4, 3.0 Hz), 1.11−1.00 (m, 42 H); ^{13}C NMR ($CDCl_3$) δ: 162.01, 159.93, 156.81, 153.89, 137.52, 133.17, 126.19, 101.50, 88.90, 86.08, 72.32, 63.32, 41.13, 18.02, 17.91, 12.13, 11.86. Anal. Calcd. for $C_{31}H_{55}N_7O_3Si_2$: C, 59.10; H, 8.80; N, 15.56. Found: C, 59.00; H, 8.75; N, 15.37.

4,7-Diamino-1-(2-deoxy-β-D-ribofuranosyl)imidazo[5′,4′:4,5]-pyrido[2,3-*d*]pyrimidine (1). To a solution of **11** (100 mg, 0.16 mmol) in THF (15 mL) was added TBAF (1 M, 0.4 mL, 0.4 mmol) at 0 °C, and the reaction mixture was stirred at room temperature for 1.5 h. After addition of AcOH (23 μL, 0.4 mmol), the solvent was removed in vacuo, and the residue was partitioned between H_2O and $CHCl_3$. The separated aqueous layer was washed with AcOEt and concentrated in vacuo. The residue was coevaporated with EtOH, and a mixture of acetone-EtOH (5:1, 5 mL) was added to the resulting solid. The suspension was heated in a water bath and then cooled to room temperature. The precipitate was collected and washed with EtOH to give **1** (45 mg, 88% as a white powder): FAB-LRMS *m*/*z* 318 (MH^+); UV λmax (H_2O) 341 nm (ε = 12 800), 254 nm (ε = 28 700), 232 nm (ε = 37 600); λmax (0.5 N HCl) 353 nm (ε = 10 800), 249 nm (ε = 42 400); λmax (0.5 N NaOH) 341 nm (ε = 12 600), 255 nm (ε = 31 400), 231 nm (ε = 41 400); ^{1}H NMR (DMSO-d_6) δ: 8.95 (s, 1 H), 8.38 (s, 1 H), 7.19 and 6.41 (each br s, each 2 H), 6.53 (t, 1 H, *J* = 6.0 Hz), 5.40 (d, 1 H, *J* = 6.9 Hz), 4.90 (t, 1 H, *J* = 5.1 Hz), 4.39 (dddd, 1 H, *J* = 6.9, 6.6, 5.2, 3.1 Hz), 3.94 (ddd, 1 H, *J* = 3.1, 4.3, 4.2 Hz), 3.51 (ddd, 1 H, *J* = 5.1, 4.3, 11.8 Hz), 3.47 (ddd, 1 H, *J* = 5.1, 4.2, 11.8 Hz), 2.72 (ddd, 1 H, *J* = 6.0, 13.2, 6.6 Hz), 2.47 (ddd, 1 H, *J* = 6.0, 13.2, 5.2 Hz); ^{13}C NMR (DMSO-d_6) δ: 162.2, 159.6, 156.7, 153.4, 138.3, 132.4, 125.2, 100.0, 87.9, 85.4, 69.9, 61.0. Anal. Calcd. for $C_{13}H_{15}N_7O_3 \cdot 3/5H_2O \cdot 1/10EtOH$: C, 47.65; H, 5.09; N, 29.47. Found: C, 47.83; H, 4.85; N, 29.35.

5-(2-Amino-4-methoxypyrimidin-5-yl)-1-(2-deoxy-3,5-di-*O*-triisopropylsilyl-β-D-ribofuranosyl)imidazole-4-carbonitrile (12). In the similar manner as described for **10**, a mixture of **5** (3.40 g, 5.25 mmol) and **8** (4.35 g, 10.5 mmol) was treated with $dba_3Pd_2 \cdot CHCl_3$ (540 mg, 0.52 mmol) to give **12** (2.75 g, 81% as a white foam): FAB-LRMS *m*/*z* 645 (MH^+); ^{1}H NMR ($CDCl_3$) δ: 8.12 and 7.99 (each s, each 1 H), 5.69 (dd, 1 H, *J* = 7.7, 5.9 Hz), 5.21 (br s, 2 H), 4.68 (ddd, 1 H, *J* = 5.2, 2.7, 1.6 Hz), 3.99 (m, 1 H), 3.91 (s, 3 H), 3.87 (m, 2 H), 2.36 (ddd, 1 H, *J* = 7.7, 13.1, 5.2 Hz), 2.31 (ddd, 1 H, *J* = 5.9, 13.1, 2.7 Hz), 1.08−1.04 (m, 42 H); ^{13}C NMR ($CDCl_3$) δ: 167.43, 163.92, 160.00, 137.00, 134.16, 114.95, 113.98, 97.62, 88.74, 85.76, 72.61, 63.50, 53.80, 43.55, 18.00, 17.95, 12.06, 11.92. Anal. Calcd. for $C_{32}H_{56}N_6O_4Si_2$: C, 59.59; H, 8.75; N, 13.03. Found: C, 59.73; H, 8.77; N, 13.11.

5-(2-Amino-4-methoxypyrimidin-5-yl)-1-(2-deoxy-3,5-di-*O*-triisopropylsilyl-β-D-ribofuranosyl)imidazole-4-carboxamide (13). To a solution of **12** (1.99 g, 3.55 mmol) in MeOH (80 mL) was added H_2O_2 (35%, 4 mL, 35.5 mmol) and NH_4OH (28%, 40 mL), and the whole mixture was stirred at room temperature for 13 h. After addition of saturated aqueous $Na_2S_2O_3$ (5 mL), the solvent was removed in vacuo, and the residue was partitioned between $CHCl_3$ and H_2O. The separated organic layer was washed with H_2O, followed by brine. The organic layer was dried (Na_2SO_4) and concentrated in vacuo. The residue was purified by a silica gel column and eluted with 0−5% MeOH in $CHCl_3$, to give **13** (1.89 g, 92% as a white foam): FAB-LRMS *m*/*z* 663 (MH^+); ^{1}H NMR ($CDCl_3$) δ: 8.17 (s, 2/3 H), 8.05 (s, 1/3 H), 7.87 (s, 1/3 H), 7.86 (s, 2/3 H), 7.01 and 5.24 (each br s, each 1 H), 5.77 (dd, 1/3 H, *J* = 7.4, 6.0 Hz), 5.60 (dd, 2/3 H, *J* = 8.0, 5.6 Hz), 5.12 (br s, 4/3 H), 5.10 (br s, 2/3 H), 4.70 (m, 2/3 H), 4.58 (m, 1/3 H), 4.03 (m, 1/3 H), 3.93 (m, 2/3 H), 3.89−3.82 (m, 2 H), 3.87 (s, 1 H), 3.84 (s, 2 H), 2.41 (ddd, 2/3 H, *J* = 8.0, 12.9, 5.3 Hz), 2.34 (ddd, 2/3 H, *J* = 5.6, 12.9, 2.3 Hz), 2.08−2.06 (m, 2/3 H), 1.09−1.00 (m, 42 H). Anal. Calcd. for $C_{32}H_{58}N_6O_5Si_2$: C, 57.97; H, 8.82; N, 12.68. Found: C, 57.92; H, 8.88; N, 12.55.

5-[4-Methoxypyrimidin-2(1*H*)-on-5-yl]-1-(2-deoxy-3,5-di-*O*-triisopropylsilyl-β-D-ribofuranosyl)imidazole-4-carboxamide (14). To a solution of **13** (1.58 g, 2.39 mmol) in THF-H_2O (70−0.7 mL) was added isoamyl nitrite (3.2 mL, 23.9 mmol) at 60 °C, and the mixture was stirred at the same temperature. After 1.5 h, an additional isoamyl nitrite (0.8 mL, 6.0 mmol) was added to the reaction mixture, and the mixture was stirred for additional 1.5 h. The reaction mixture was neutralized by addition of saturated aqueous $NaHCO_3$, and the solvent was removed in vacuo. The residue was partitioned between AcOEt and H_2O, and the separated organic layer was washed with H_2O, followed by brine. The organic layer was dried (Na_2SO_4) and concentrated in vacuo. The residue was purified by a silica gel column and eluted with 0−10% EtOH in $CHCl_3$, to give **14** (804 mg, 51% as a white foam): FAB-LRMS *m*/*z* 664 (MH^+); ^{1}H NMR ($CDCl_3$) δ: 12.07 (br s, 1/3 H), 11.75 (br s, 2/3 H), 7.91 (s, 1/3 H), 7.88 and 7.80 (each s, each 2/3 H), 7.72 (s, 1/3 H), 7.11 and 5.89 (each br s, each 1/3 H), 7.07 and 5.80 (each br s, each 2/3 H), 5.64 (m, 1 H), 4.72 (m, 2/3 H), 4.64 (m, 1/3 H), 4.05−3.82 (m, 3 H), 3.96 (s, 1 H), 3.94 (s, 2 H), 2.48 (ddd, 2/3 H, *J* = 7.3, 13.1, 5.5 Hz), 2.34 (m, 2/3 H), 2.17 (m, 1/3 H), 2.11 (m, 1/3 H), 1.09−1.03 (m, 42 H). Anal. Calcd. for $C_{32}H_{57}N_5O_6Si_2$: C, 57.88; H, 8.65; N, 10.55. Found: C, 57.62; H, 8.60; N, 10.44.

1-(2-Deoxy-3,5-di-*O*-triisopropylsilyl-β-D-ribofuranosyl)imidazo-[5′,4′:4,5]pyrido[2,3-*d*]pyrimidine-4,7(5*H*,6*H*)-dione (15). A solution of **14** (800 mg, 1.20 mmol) in methanolic ammonia (saturated at 0 °C, 40 mL) was heated at 120 °C for 48 h in a steel container. The solvent was removed in vacuo, and the residue was crystallized from EtOH-$CHCl_3$ to give **15** (553 mg, 73%): mp >300 °C; FAB-LRMS *m*/*z* 632 (MH^+); ^{1}H NMR (DMSO-d_6) δ: 12.16 and 11.68 (each br s, each 1 H), 8.45 (s, 1 H), 8.21 (s, 1 H), 6.41 (dd, 1 H, *J* = 5.4, 4.9 Hz), 4.70 (ddd, 1 H, *J* = 5.0, 7.3, 4.3 Hz), 3.95 (ddd, 1 H, *J* = 4.3, 3.8, 4.1 Hz), 3.74 (dd, 1 H, *J* = 3.8, 11.4 Hz), 3.59 (dd, 1 H, *J* = 4.1, 11.4 Hz), 3.04 (ddd, 1 H, *J* = 5.4, 13.1, 5.0 Hz), 2.50 (ddd, 1 H, *J* = 4.9, 13.1, 7.3 Hz), 1.05−0.84 (m, 42 H); ^{13}C NMR (DMSO-d_6) δ: 158.1, 138.2, 132.0, 129.4, 87.9, 84.5, 70.8, 62.2, 38.6, 17.6, 17.3, 11.6, 11.2. Anal. Calcd. for $C_{31}H_{53}N_5O_5Si_2$: C, 58.92; H, 8.45; N, 11.08. Found: C, 59.02; H, 8.45; N, 11.16.

1-(2-Deoxy-β-D-ribofuranosyl)imidazo[5′,4′:4,5]pyrido[2,3-*d*]-pyrimidine-4,7(5*H*,6*H*)-dione (2). To a solution of **15** (115 mg, 0.18 mmol) in THF (15 mL) was added TBAF (1 M, 0.45 mL, 0.45 mmol) at 0 °C, and the reaction mixture was stirred at room temperature for 1.5 h. After addition of AcOH (26 μL, 0.45 mmol), the solvent was removed in vacuo, and the residue was partitioned between H_2O and $CHCl_3$. The separated aqueous layer was washed with AcOEt and concentrated in vacuo. The residue was coevaporated with EtOH, and a mixture of EtOH-H_2O (4:1, 5 mL) was added to the resulting solid. The suspension was heated in a water bath and then cooled to room temperature. The precipitate was collected and washed with EtOH to give **2** (51 mg, 89% as a white powder): FAB-LRMS *m*/*z* 320 (MH^+); UV λmax (H_2O) 338 nm (ε = 9700), 243 nm (ε = 35 000); λmax (0.5 N HCl) 330 nm (ε = 10 000), 241 nm (ε = 29 200); λmax (0.5 N NaOH) 339 nm (ε = 14 000), 254 nm (ε = 26 900); ^{1}H NMR (DMSO-d_6) δ: 12.09 and 11.61 (each br s, each 1 H), 8.45 (s, 1 H), 8.29 (s, 1 H), 6.35 (dd, 1 H, *J* = 6.0, 5.7 Hz), 5.36 (d, 1 H, *J* = 4.7 Hz), 4.78 (t,

1 H, J = 5.0 Hz), 4.38 (dddd, 1 H, J = 4.7, 6.3, 5.3, 2.8 Hz), 3.92 (ddd, 1 H, J = 2.8, 4.7, 4.8 Hz), 3.46 (ddd, 1 H, J = 5.0, 4.7, 11.8 Hz), 3.39 (ddd, 1 H, J = 5.0, 4.8, 11.8 Hz), 2.80 (ddd, 1 H, J = 6.0, 13.2, 6.3 Hz), 2.40 (ddd, 1 H, J = 5.7, 13.2, 5.3 Hz); ^{13}C NMR (DMSO-d_6) δ: 158.4, 139.0, 132.0, 129.3, 88.2, 84.9, 69.9, 61.0, 38.4. Anal. Calcd. for $C_{13}H_{13}N_5O_5$: C, 48.91; H, 4.10; N, 21.93. Found: C, 48.86; H, 4.15; N, 21.88.

5-[4-Methoxypyrimidin-2(1*H*)-on-5-yl]-1-(2-deoxy-3,5-di-*O*-triisopropylsilyl-*β*-D-ribofuranosyl)imidazole-4-carbonitrile (16). In the similar manner as described for **14**, **12** (1.68 g, 2.61 mmol) was treated with isoamyl nitrite (3.5 mL, 26.1 mmol) to give **16** (967 mg, 57% as a white foam): FAB-LRMS *m*/*z* 646 (MH^+); ^{1}H NMR ($CDCl_3$) δ: 12.31 (br s, 1 H), 8.01 and 7.79 (each s, each 1 H), 5.70 (dd, 1 H, J = 7.8, 5.7 Hz), 4.72 (dt, 1 H, J = 5.4, 2.3 Hz), 4.03 (m, 4 H,), 3.87 (m, 2 H), 2.44 (ddd, 1 H, J = 7.8, 12.8, 5.4 Hz), 2.36 (ddd, 1 H, J = 5.7, 12.8, 2.3 Hz), 1.08−1.04 (m, 42 H); ^{13}C NMR ($CDCl_3$) δ: 169.85, 158.92, 146.90, 137.74, 131.84, 115.11, 114.52, 95.77, 89.18, 85.99, 72.79, 63.64, 55.38, 43.47, 18.19, 18.15, 12.26, 12.10. Anal. Calcd. for $C_{32}H_{55}N_5O_5Si_2$: C, 59.50; H, 8.58; N, 10.84. Found: C, 59.72; H, 8.66; N, 10.68.

4-Amino-1-(2-deoxy-3,5-di-*O*-triisopropylsilyl-*β*-D-ribofuranosyl)-imidazo[5′,4′:4,5]pyrido[2,3-*d*]pyrimidin-7(6*H*)-one (17). In the similar manner as described for **15**, **16** (960 mg, 1.49 mmol) was treated with methanolic ammonia (saturated at 0 °C, 40 mL) to give **17** (882 mg, 94%, crystallized from acetone-$CHCl_3$): mp 287−289 °C; FAB-LRMS *m*/*z* 631 (MH^+); ^{1}H NMR ($CDCl_3$) δ: 13.77 (br s, 1 H), 10.30 and 6.44 (each br s, each 1 H), 9.33 (s, 1 H), 8.02 (s, 1 H), 6.42 (dd, 1 H, J = 7.9, 5.2 Hz), 4.82 (ddd, 1 H, J = 5.0, 2.8, 1.6 Hz), 4.22 (ddd, 1 H, J = 1.6, 2.6, 3.7 Hz), 3.88 (dd, 1 H, J = 2.6, 11.3 Hz), 3.83 (dd, 1 H, J = 3.7, 11.3 Hz), 2.70 (ddd, 1 H, J = 7.9, 12.7, 5.0 Hz), 2.62 (ddd, 1 H, J = 5.2, 12.7, 2.8 Hz), 1.12−0.99 (m, 42 H); ^{13}C NMR ($CDCl_3$) δ: 160.38, 159.06, 157.45, 153.53, 137.92, 133.40, 125.15, 96.31, 89.07, 85.95, 72.35, 63.15, 40.99, 18.00, 17.86, 12.10, 11.81. Anal. Calcd. for $C_{31}H_{54}N_6O_4Si_2$: C, 59.01; H, 8.63; N, 13.32. Found: C, 58.92; H, 8.56; N, 13.30.

4-Amino-1-(2-deoxy-*β*-D-ribofuranosyl)imidazo[5′,4′:4,5]pyrido-[2,3-*d*]pyrimidin-7(6*H*)-one (3). In the similar manner as described for **2**, **17** (220 mg, 0.35 mmol) was treated with TBAF (1 M, 0.88 mL, 0.88 mmol) to give **3** (83 mg, 74% as a white powder): FAB-LRMS *m*/*z* 319 (MH^+); UV λmax (H_2O) 348 nm (ϵ = 17 900), 252 nm (ϵ = 24 000); λmax (0.5 N HCl) 356 nm (ϵ = 17 400), 304 nm (ϵ = 8300), 244 nm (ϵ = 18 700); λmax (0.5 N NaOH) 344 nm (ϵ = 12 600), 252 nm (ϵ = 29 700); ^{1}H NMR (DMSO-d_6) δ: 11.74 (br s, 1 H), 9.09 (s, 1 H), 8.39 (s, 1 H), 7.78 (br s, 2 H), 6.52 (dd, 1 H, J = 6.1, 6.0 Hz), 5.37 (d, 1 H, J = 4.5 Hz), 4.85 (t, 1 H, J = 4.9 Hz), 4.39 (dddd, 1 H, J = 4.5, 6.6, 5.0, 3.4 Hz), 3.95 (ddd, 1 H, J = 3.4, 4.0, 4.8 Hz), 3.51 (ddd, 1 H, J = 4.9, 4.0, 11.8 Hz), 3.46 (ddd, 1 H, J = 4.9, 4.8, 11.8 Hz), 2.75 (ddd, 1 H, J = 6.1, 13.2, 6.6 Hz), 2.48 (ddd, 1 H, J = 6.0, 13.2, 5.0 Hz); ^{13}C NMR (DMSO-d_6) δ: 159.5, 156.8, 156.3, 152.8, 138.8, 133.0, 123.9, 94.7, 87.9, 85.4, 69.9, 61.0. Anal. Calcd. for $C_{13}H_{14}N_6O_4 \cdot 1/3H_2O$: C, 48.15; H, 4.56; N, 25.91. Found: C, 48.26; H, 4.49; N, 25.67.

1-(2-Deoxy-3,5-di-*O*-triisopropylsilyl-*β*-D-ribofuranosyl)-5-iodo-imidazole-4-[*N*,*N*-di-(*tert*-butoxycarbonyl)]carboxamide (18). To a solution of **6** (3.5 g, 5.26 mmol) in CH_2Cl_2 (60 mL) containing Et_3N (2.2 mL, 15.8 mmol) and DMAP (640 mg, 5.26 mmol) was added di-*tert*-butyl dicarbonate (3.6 mL, 15.8 mmol), and the whole mixture was stirred at room temperature. After 10 h, an additional di-*tert*-butyl dicarbonate (1.8 mL, 7.9 mmol) was added to the reaction mixture. After an additional 10 h, the solvent was removed in vacuo, and the residue was purified by a silica gel column and eluted with hexane/AcOEt (20:1−6:1), to give **18** (4.32 g, 95% as a colorless oil): FAB-LRMS *m*/*z* 866 (MH^+); FAB-HRMS calcd. for $C_{37}H_{69}IN_3O_8Si_2$ 866.3669, found: 866.3685. ^{1}H NMR ($CDCl_3$) δ: 8.04 (s, 1 H), 6.13 (dd, 1 H, J = 5.4, 8.1 Hz), 4.68 (ddd, 1 H, J = 2.3, 5.2, 2.6 Hz), 4.10 (m, 1 H), 3.91 (m, 2 H), 2.50 (ddd, 1 H, J = 5.4, 12.8, 2.3 Hz), 2.22 (ddd, 1 H, J = 8.1, 12.8, 5.2 Hz), 1.10−1.05 (m, 42 H); ^{13}C NMR ($CDCl_3$) δ: 163.05, 149.79, 137.79, 88.81, 88.68, 83.29, 81.67, 76.86, 72.36, 63.14, 43.38, 27.84. 27.50, 17.79, 11.88, 11.66.

Methyl 1-(2-Deoxy-3,5-di-*O*-triisopropylsilyl-*β*-D-ribofuranosyl)-5-iodoimidazole-4-carboxylate (19). To a solution of **18** (4.2 g, 4.86 mmol) in MeOH (70 mL) was added 28% NaOMe (2 mL, 9.8 mmol), and the whole mixture was stirred at room temperature for 3 h. The reaction was quenched by addition of saturated aqueous NH_4Cl, and the solvent was removed in vacuo. The residue was partitioned between AcOEt and H_2O. The separated organic layer was washed with H_2O, followed by brine. The organic layer was dried (Na_2SO_4), and concentrated in vacuo. The residue was purified by a silica gel column and eluted with hexane/AcOEt (9:1−2:1), to give **19** (3.24 g, 98%, crystallized from hexane): mp 90−91 °C; FAB-LRMS *m*/*z* 681 (MH^+); ^{1}H NMR ($CDCl_3$) δ: 8.10 (s, 1 H), 6.14 (dd, 1 H, J = 5.5, 7.9 Hz), 4.69 (ddd, 1 H, J = 2.4, 5.2, 1.6 Hz), 4.11 (m, 1 H), 3.92 (m, 2 H), 2.50 (ddd, 1 H, J = 5.5, 12.9, 2.4 Hz), 2.22 (ddd, 1 H, J = 7.9, 12.9, 5.2 Hz), 1.10−1.05 (m, 42 H); ^{13}C NMR ($CDCl_3$) δ: 162.75, 138.58, 135.65, 89.11, 88.93, 76.43, 72.72, 63.38, 51.77, 43.54, 17.95, 12.06, 11.84. Anal. Calcd. for $C_{28}H_{53}IN_2O_5Si_2$: C, 49.40; H, 7.85; N, 4.11. Found: C, 49.19; H, 7.82; N, 4.04.

7-Amino-1-(2-deoxy-3,5-di-*O*-triisopropylsilyl-*β*-D-ribofuranosyl)-imidazo[5′,4′:4,5]pyrido[2,3-*d*]pyrimidin-4(5*H*)-one (22). In the similar manner as described for **11**, a mixture of **19** (3.38 g, 4.97 mmol) and **7** (3.12 g, 7.46 mmol) was treated with $dba_3Pd_2 \cdot CHCl_3$ (414 mg, 0.40 mmol) to give a brown syrup. The resulting crude mixture was then dissolved in 1,4-dioxane (30 mL), and NH_4OH (28%, 30 mL) was added to the mixture. The whole was heated at 100 °C for 60 h in a steel container. The solvent was removed in vacuo, and the residue was partitioned between $CHCl_3$ and H_2O. The separated organic layer was washed with H_2O, followed by brine. The organic layer was dried (Na_2SO_4) and concentrated in vacuo. The residue was purified by a silica gel column and eluted with 0−5% EtOH in $CHCl_3$, to give **22** (1.78 g, 57%, crystallized from acetone-$CHCl_3$): mp 187−188 °C; FAB-LRMS *m*/*z* 631 (MH^+); ^{1}H NMR ($CDCl_3$) δ: 12.90 (br s, 1 H), 9.05 (s, 1 H), 7.96 (s, 1 H), 6.41 (dd, 1 H, J = 7.7, 5.2 Hz), 4.82 (ddd, 1 H, J = 5.1, 2.9, 1.0 Hz), 4.20 (ddd, 1 H, J = 1.0, 2.9, 4.0 Hz), 3.86 (dd, 1 H, J = 2.9, 11.2 Hz), 3.80 (dd, 1 H, J = 4.0, 11.2 Hz), 2.73 (ddd, 1 H, J = 7.7, 12.4, 5.1 Hz), 2.63 (ddd, 1 H, J = 5.2, 12.4, 2.9 Hz), 1.12−0.98 (m, 42 H); ^{13}C NMR ($CDCl_3$) δ: 162.18, 160.13, 154.56, 154.44, 137.93, 133.88, 129.81, 98.03, 89.09, 85.79, 72.48, 63.29, 40.76, 18.05, 17.90, 12.15, 11.85. Anal. Calcd. for $C_{31}H_{54}N_6O_4Si_2$: C, 59.01; H, 8.63; N, 13.32. Found: C, 59.06; H, 8.59; N, 13.24.

7-Amino-1-(2-deoxy-*β*-D-ribofuranosyl)imidazo[5′,4′:4,5]pyrido-[2,3-*d*]pyrimidin-4(5*H*)-one (4). In the similar manner as described for **2**, **22** (255 mg, 0.40 mmol) was treated with TBAF (1 M, 1.0 mL, 1.0 mmol) to give **4** (103 mg, 81% as a white powder): FAB-LRMS *m*/*z* 319 (MH^+); UV λmax (H_2O) 333 nm (ϵ = 14 400), 281 nm (ϵ = 10 900), 240 nm (ϵ = 28 700); λmax (0.5 N HCl) 330 nm (ϵ = 8500), 244 nm (ϵ = 33 300); λmax (0.5 N NaOH) 337 nm (ϵ = 13 900), 257 nm (ϵ = 26 200); ^{1}H NMR (DMSO-d_6) δ: 11.52 (br s, 1 H), 8.85 (s, 1 H), 8.30 (s, 1 H), 6.89 (br s, 2 H), 6.47 (t, 1 H, J = 6.0 Hz), 5.37 (d, 1 H, J = 5.0 Hz), 4.86 (t, 1 H, J = 5.0 Hz), 4.38 (dddd, 1 H, J = 5.0, 6.3, 4.7, 3.4 Hz), 3.93 (ddd, 1 H, J = 3.4, 4.3, 4.4 Hz), 3.51 (ddd, 1 H, J = 5.0, 4.3, 11.8 Hz), 3.45 (ddd, 1 H, J = 5.0, 4.4, 11.8 Hz), 2.72 (ddd, 1 H, J = 6.0, 13.2, 6.3 Hz), 2.45 (ddd, 1 H, J = 6.0, 13.2, 4.7 Hz); ^{13}C NMR (DMSO-d_6) δ: 161.7, 158.3, 154.3, 153.3, 138.6, 132.7, 129.3, 96.9, 87.9, 85.3, 69.8, 61.0, 39.0. Anal. Calcd. for $C_{13}H_{14}N_6O_4 \cdot 3/10H_2O \cdot 1/5EtOH$: C, 48.35; H, 4.78; N, 25.24. Found: C, 48.42; H, 4.73; N, 25.28.

Synthesis of ODNs. ODNs were synthesized on a DNA/RNA synthesizer (Applied Biosystem Model 392) by the phosphoramidite method.[34] For the incorporation of the tricyclic nucleosides into the ODNs, a 0.12 M solution of each tricyclic nucleoside phosphoramidite

(34) Beaucage, S. L.; Caruthers, M. H. *Tetrahedron Lett*. **1981**, *22*, 1859−1862.

in CH_3CN and a coupling time of 120 s was used. The fully protected ODNs were then deblocked and purified by the same procedure as for the purification of normal ODNs.[35] Thus, each ODN linked to the resin (1 μmol) was treated with concentrated NH_4OH at 55 °C for 16 h, and the released ODN protected by a DMTr group at the 5′-end was chromatographed on a C-18 silica gel column (1 × 12 cm, Waters) with a linear gradient of CH_3CN from 0 to 40% in 0.1 M TEAA buffer (pH 7.0). The fractions were concentrated, the residue was treated with aqueous 80% AcOH at room temperature for 20 min, then the solution was concentrated, and the residue was coevaporated with H_2O. The residue was dissolved in H_2O, the solution was washed with Et_2O, and then the H_2O layer was concentrated to give the deprotected ODN. The ODN was further purified by reverse-phase HPLC, using a J'sphere ODN M80 column (4.6 × 150 mm, YMC) with a linear gradient of CH_3CN (from 10 to 25% over 30 min) in 0.01 M TEAA buffer (pH 7.0) to give highly purified ODNs.

Complete Hydrolysis of the ODNs. Each ODN (0.2 OD units at 260 nm) was incubated with snake venom phosphodiesterase (10 μg), nuclease P1 (10 μg), and alkaline phosphatase (0.4 units) in a buffer containing 100 mM Tris-HCl (pH 7.7) and 2 mM $MgCl_2$ (total 125 μL) at 37 °C for 12 h. After this was heated in boiling water for 5 min, cold EtOH (320 μL) was added to the reaction mixture, and the mixture was kept at −30 °C for 1 h. The cold solution was centrifuged for 20 min (12 000 rpm), and then the supernatant was separated and concentrated. The residue was analyzed by reverse-phase HPLC, using a J'sphere ODN M80 column (4.6 × 150 mm, YMC) with a linear gradient of CH_3CN (from 2 to 12% over 40 min) in 0.01 M TEAA buffer (pH 7.0).

Hyperchromicities and Extinction Coefficients of the ODNs. Each ODN (0.25 OD units at 260 nm) was enzymatically hydrolyzed under the conditions described above. Hyperchromicity of each ODN was determined by comparing UV absorbances at 260 nm of the solutions before and after hydrolyses. The extinction coefficient (at 260 nm) of each ODN was determined using the following equation: ϵ_{ODN} = the sum of $\epsilon_{nucleoside}$/hyperchromicity. The extinction coefficients (at 260 nm) of the natural nucleosides used for calculations were as follows: dA, 15 400; dC, 7300; dG, 11 700; T, 8800. The extinction coefficients for the tricyclic nucleosides at 260 nm were determined to be the following: $\mathbf{N^N}$, 26 200; $\mathbf{O^O}$, 11 900; $\mathbf{N^O}$, 18 100; $\mathbf{O^N}$, 9400.

Thermal Denaturation. Each sample that contained appropriate ODNs in a buffer of either 0.01 M sodium cacodylate (pH 7.0) containing 0.1 M NaCl or 0.01 M sodium phosphate (pH 7.0) containing 1.0 M NaCl was heated at 95 °C for 5 min, cooled gradually to an appropriate temperature, and used for the thermal denaturation study. Thermal-induced transitions of each mixture of ODNs were monitored at 260 nm on a Perkin-Elmer Lambda 2S. The sample temperature was increased 0.5 °C/min. Thermodynamic parameters were derived by the reported method.[36]

Acknowledgment. This work was supported in part by Grant-in-Aid for Scientific Research on Priority Areas and Encouragement of Young Scientists from the Ministry of Education, Science, Sports, and Culture of Japan. We would like to thank Ms. H. Matsumoto and Ms. A. Maeda (Center for Instrumental Analysis, Hokkaido University) for elemental analysis. We also would like to thank Ms. S. Oka (Center for Instrumental Analysis, Hokkaido University) for measurement of mass spectra. This paper constitutes Part 222 of Nucleosides and Nucleotides. Part 221 is ref 37.

Supporting Information Available: Experimental details of synthesis of **5** and **6** (SI−Scheme 1), **7** and **8** (SI−Scheme 2), phosporamidites (SI−Scheme 3), **23** (SI−Scheme 4), SI−Figure 1 (^{1}H NMR spectra of homodimer **17·17**), SI−Figure 2 (^{1}H NMR spectra of a mixture of **17** and **22**), SI−Figure 3 (^{1}H NMR spectra of a mixture of **11** and **15**), enzymatic digestion of ODNs (SI−Figure 4 and SI−Table 1), thermodynamic parameters of the duplexes containing the tricyclic nucleosides (SI−Tables 2 and 3). This material is available free of charge via the Internet at http://pubs.acs.org.

JA0347686

(35) Gait, M. L., Ed. *Oligonucleotides synthesis: a practical approach*; IRL Press: Oxford, UK, 1984.

(36) Marky, L. A.; Breslaure, K. L. *Biopolymer* **1987**, *26*, 1601−1620.

(37) Itoh, T.; Ueno, Y.; Komatsu, Y.; Matsuda, A. *Nucleic Acids Res*. **2003**, *31*, 2514−2523.